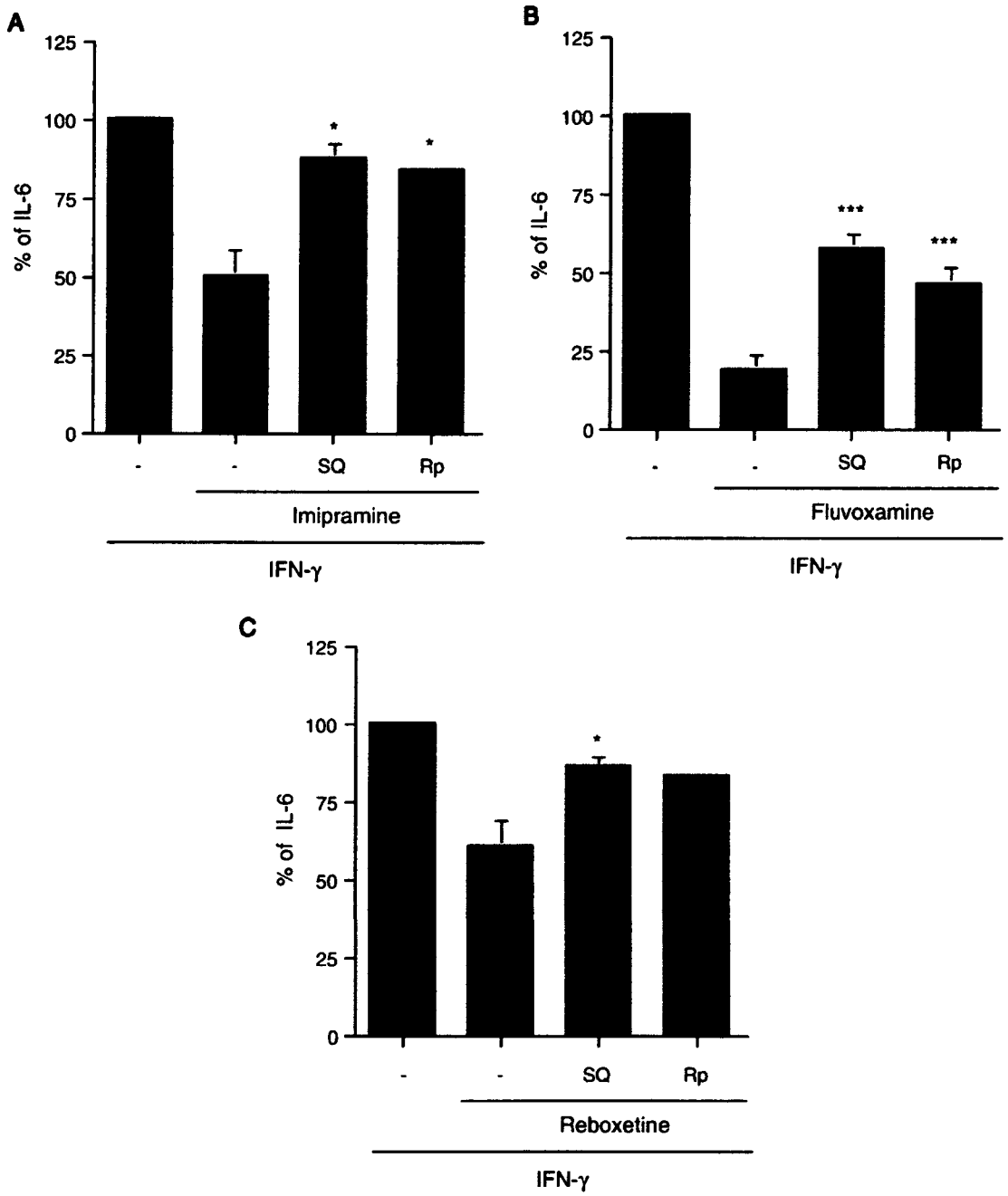

Fig. 4. Effects of cAMP/PKA inhibitors on the antidepressants-induced IL-6 suppression. 6-3 microglial cells were pre-incubated for 20 min with SQ 22536 (10 μM) or Rp-3′,5′-cAMPS (10 μM) before the addition of imipramine (50 μM) (A), fluvoxamine (50 μM) (B) or reboxetine (50 μM) (C). After 24 h of the pretreatment with antidepressants, the cells were stimulated by 100 U/ml of IFN-γ. After 24 h, the media collected were assayed for IL-6 accumulation using ELISA. Values are the means±SEM of 3–6 samples and expressed as percentage control, where 100% is the value obtained from IFN-γ alone. *$p<0.05$, ***$p<0.0001$, compared with imipramine (A), fluvoxamine (B) or reboxetine (C). Comparisons were made with ANOVA followed by the Fisher's PLSD. SQ, SQ 22536; Rp, Rp-3′,5′-cAMPS.

significantly those antidepressants-induced suppression of IL-6. In the case of reboxetine, the effect reached significance for SQ 22536 but only a non-significant trend was observed for Rp-3′,5′-cAMPS (Fig. 4C, $p=0.0558$).

Effects of cAMP/PKA inhibitors on the antidepressants-induced NO suppression

Finally, we investigated the effects of SQ 22536 and Rp-3′,5′-cAMPS on antidepressant or lithium chloride-induced NO suppression. We observed that 10 μM of SQ 22536 alone did not affect significantly the IFN-γ-induced microglial NO production, whereas 10 μM of Rp-3′,5′-cAMPS alone decreased significantly the IFN-γ-induced microglial NO production to 83.1±2.1% (data not shown).

Fig. 5 shows that both SQ 22536 and Rp-3′,5′-cAMPS at a dose of 10 μM significantly reversed the inhibitory effects of antidepressants on the IFN-γ-induced increase of microglial NO production. The effect is shown for imipramine (Fig. 5A), fluvoxamine (Fig. 5B) and reboxetine (Fig. 5C) tested at a dose

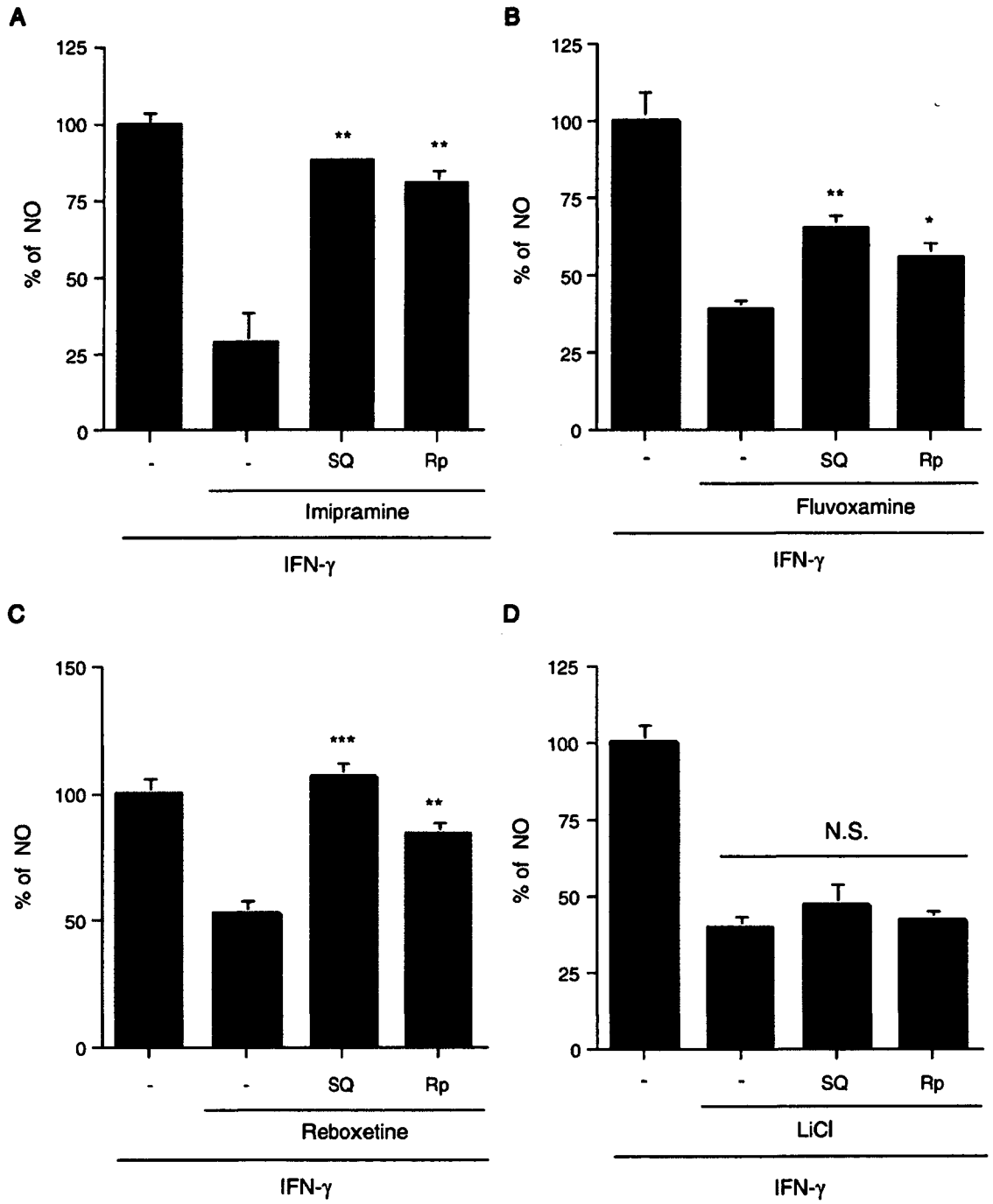

Fig. 5. Effects of cAMP/PKA inhibitors on the antidepressants-induced NO suppression. 6-3 microglial cells were pre-incubated for 20 min with SQ 22536 (10 μM) or Rp-3′,5′-cAMPS (10 μM) before the addition of imipramine (50 μM) (A), fluvoxamine (50 μM) (B), reboxetine (50 μM) (C) or lithium chloride (1 mM) (D). After 24 h of the pretreatment with antidepressants or lithium chloride, the cells were stimulated by 100 U/ml of IFN-γ. After 48 h, the media collected were assayed for NO accumulation using Griess reaction. Values are the means±SEM of 3–6 samples and expressed as percentage control, where 100% is the value obtained from IFN-γ alone. $*p<0.05$, $**p<0.01$, $***p<0.0001$, compared with imipramine (A), fluvoxamine (B), reboxetine (C) or lithium chloride (D). Comparisons were made with ANOVA followed by the Fisher's PLSD. N.S., no significance; SQ, SQ 22536; Rp, Rp-3′,5′-cAMPS.

of 50 μM. In contrast, SQ 22536 and Rp-3′,5′-cAMPS did not reverse the lithium chloride-induced NO suppression (Fig. 5D).

Discussion

Our study had four major findings. First, various types of antidepressants inhibited the IFN-γ-induced microglial production of inflammatory mediators such as IL-6 and NO. Second, these inhibitions were reversed significantly by either a cAMP inhibitor (SQ 22536) or a PKA inhibitor (Rp-3′,5′-cAMPS). Third, lithium chloride enhanced the IFN-γ-induced microglial production of IL-6, while it inhibited the production of NO. Fourth, the lithium chloride-induced NO suppression was not reversed by either SQ 22536 or Rp-3′,5′-cAMPS.

In line with the recent *ex vivo/in vitro* studies demonstrating the immunosuppressive effects of antidepressants (Kubera et al., 2001; Maes et al., 1999, 2005; Obuchowicz et al., 2006; Szuster-Ciesielska et al., 2003; Xia et al., 1996), the present study has shown that various types of antidepressants inhibit the IFN-γ-induced microglial production of both IL-6 and NO. The detailed mechanism by which antidepressants inhibit the production of pro-inflammatory mediators by immune cells, including microglia, still remains to be elucidated. However, several *ex vivo/in vitro* studies have suggested that elevated intracellular cAMP concentrations, induced by treatment with antidepressants (Xia et al., 1996), contribute to the immunosuppressive effects of antidepressants (Kubera et al., 2001; Maes et al., 2005). Consistent with these studies, our results have demonstrated that SQ 22536 and Rp-3′,5′-cAMPS reverse significantly the antidepressant-induced inhibition of microglial IL-6 and NO production. The only exception was that the effect of Rp-3′,5′-cAMPS did not reach significance for reboxetine at the concentrations used ($p=0.0558$). These results suggest that the inhibitory effects of antidepressants on IFN-γ-activated microglia are, at least partially, mediated by the cAMP-dependent PKA pathway. Indeed, in a number of cell types, the activation of cAMP/PKA pathway has been shown to inhibit the transcription factor nuclear factor-κB (Delfino and Walker, 1999), whose activation is known to induce the gene expression of inducible NO synthase and various pro-inflammatory cytokines, including IL-6 (Yoshimura, 2006).

A number of *in vivo* studies have suggested that many antidepressants increase intracellular levels of cAMP through activation of monoamine receptors such as the receptors for serotonin (5-HT), noradrenaline (NA) (Duman, 1998; Malberg and Blendy, 2005) and dopamine (Brustolim et al., 2006). Explicitly, the majority of antidepressants increase synaptic levels of 5-HT and NA through inhibiting reuptake by their transporters on presynaptic neurons, and thus cause the activation of their receptors coupled to G-proteins that can regulate the cAMP system. Through G-protein activation of adenylate cyclase (i.e., through the activation of 5-HT or NA receptor subtypes positively coupled to adenylate cyclase), cAMP production is increased. Our *in vitro* study suggests that antidepressants may have an action on microglia independently of such receptors. They may act in a monoamine receptor-independent manner. Alternatively, they may act on interferon-γ receptors or other unidentified surface receptors that are linked to G proteins. We also cannot rule out direct effects of antidepressants on G proteins.

There are also reports of pro-inflammatory effects of antidepressants, suggesting an opposite mechanism of action to our study. Specifically, it has been shown that imipramine enhances IL-6 production in human whole blood stimulated with phytohemagglutinin/LPS (Kubera et al., 2004) and that fluoxetine increases the IL-6, NO and TNF-α production when applied to unstimulated BV2 murine microglial cells (Ha et al., 2006). The effects of antidepressants on the production of pro-inflammatory mediators may therefore depend on the type of G proteins stimulated.

Another possible target of antidepressants in microglia is the phosphodiesterase (PDE) that degrades cAMP. Recently, PDE genes have been shown to be associated with a susceptibility to major depression and antidepressant treatment response (Wong et al., 2006). Accordingly, antidepressants could directly affect PDE function in microglia *in vitro* and thus increase the intracellular cAMP.

IC_{50} values of imipramine and fluvoxamine for inhibiting [^{3}H]5-HT uptake into rat cortical synaptosomes have been reported to be 500 nM and 70 nM, respectively (Inazu et al., 2001). In addition, IC_{50} values of reboxetine for inhibiting [^{3}H]NA and [^{3}H]5-HT uptake into rat hippocampal synaptosomes have been shown to be 8.5 nM and 6.9 μM, respectively (Miller et al., 2002). Compared with above-mentioned values, IC_{50} values of imipramine, fluvoxamine and reboxetine as inhibitors of microglial IL-6 production, which were calculated to be 37.0 μM, 25.6 μM and 51.5 μM, respectively, in the present study, appear to be high. The discrepancy between the aforementioned values and ours might stem from differences in the cell type and species. The other possibility is that, at the doses used for this study, antidepressants could act on some molecules other than monoamine transporters. In that case, G protein seems to be one of the potential targets of antidepressants in microglia as mentioned above.

The effects of lithium chloride on IFN-γ-induced microglial production of pro-inflammatory mediators differed considerably from antidepressants, as it enhanced IL-6 production and inhibited NO production. Our results are consistent with other studies demonstrating that lithium increased the production of pro-inflammatory cytokines such as IL-6 and TNF-α in human monocytes (Arena et al., 1997; Merendino et al., 1994). However, we demonstrated a paradoxical effect of lithium chloride in that it inhibited NO production. This inhibition was not reversed by either a cAMP inhibitor or a PKA inhibitor. These results suggest that the inhibitory effect of lithium on the microglial NO production is not mediated by the cAMP-dependent PKA pathway. Based on the dual effects of lithium chloride on microglial production of pro-inflammatory mediators, the mechanism of lithium action on IFN-γ-activated microglia appears to be complicated and needs further validation.

Several stimulants such as IFN-γ, LPS and PMA are well known to activate microglial cells. Most importantly, IFN-γ has been associated with major depression. Maes et al. (1994) have demonstrated that the IFN-γ secretion by mitogen-stimulated PBMC from patients with major depression is significantly higher than that from healthy subjects. In addition, IFN-γ has been shown to induce such depression-like behavior as decreased locomotor activity in mice (Weinberger et al., 1988). Accordingly, our experimental method using IFN-γ seems to be consistent with a possible pathophysiologic microenvironment in the brain of depressed patients.

Unlike IL-6, which has been shown to act as an inhibitory regulator of neurogenesis, NO has been indicated to have a dual role in adult neurogenesis (Cardenas et al., 2005). According to *in vivo* studies, NO produced by neuronal NO synthase (NOS) decreases neurogenesis (Moreno-Lopez et al., 2004), whereas

NO synthesized from inducible NOS and endothelial NOS stimulates neurogenesis (Reif et al., 2004; Zhu et al., 2003). NO under neuroinflammatory conditions has been shown to decrease neurogenesis *in vitro* (Covacu et al., 2006). Therefore, the precise role of NO in adult neurogenesis remains unclear. In this study NO production was used as a reliable parameter of rodent microglial activation.

In conclusion, this study demonstrates that various types of antidepressants inhibit IFN-γ-induced microglial production of pro-inflammatory mediators such as IL-6 and NO, while lithium chloride has mixed effects. The antidepressants-induced inhibitions seem to be, at least partially, mediated by the cAMP-dependent PKA pathway. These results support the view that antidepressants can inhibit microglial activation *in vitro*, raising the possibility that antidepressants indirectly promote adult neurogenesis through the inhibition of activated microglia *in vivo*.

Acknowledgments

Sincere appreciation is extended to Dr. Yoshito Mizoguchi and Dr. Tetsuaki Arai for their valuable advice and kind support. This research was supported in part by the Pacific Alzheimer Research Foundation.

References

Arena, A., Capozza, A.B., Orlando, M.E., Curro, F., Losi, E., Chillemi, S., Mesiti, M., Merendino, R.A., 1997. In vitro effects of lithium chloride on TNF alpha and IL-6 production by monocytes from breast cancer patients. J. Chemother. 9, 219–226.

Brustolim, D., Ribeiro-dos-Santos, R., Kast, R.E., Altschuler, E.L., Soares, M.B., 2006. A new chapter opens in anti-inflammatory treatments: the antidepressant bupropion lowers production of tumor necrosis factor-alpha and interferon-gamma in mice. Int. Immunopharmacol. 6, 903–907.

Cardenas, A., Moro, M.A., Hurtado, O., Leza, J.C., Lizasoain, I., 2005. Dual role of nitric oxide in adult neurogenesis. Brain Res. Brain Res. Rev. 50, 1–6.

Castanon, N., Leonard, B.E., Neveu, P.J., Yirmiya, R., 2002. Effects of antidepressants on cytokine production and actions. Brain Behav. Immun. 16, 569–574.

Covacu, R., Danilov, A.I., Rasmussen, B.S., Hallen, K., Moe, M.C., Lobell, A., Johansson, C.B., Svensson, M.A., Olsson, T., Brundin, L., 2006. Nitric oxide exposure diverts neural stem cell fate from neurogenesis towards astrogliogenesis. Stem Cells 24, 2792–2800.

De La Garza 2nd, R., 2005. Endotoxin- or pro-inflammatory cytokine-induced sickness behavior as an animal model of depression: focus on anhedonia. Neurosci. Biobehav. Rev. 29, 761–770.

Delfino, F., Walker, W.H., 1999. Hormonal regulation of the NF-κB signaling pathway. Mol. Cell. Endocrinol. 157, 1–9.

Duman, R.S., 1998. Novel therapeutic approaches beyond the serotonin receptor. Biol. Psychiatry 44, 324–335.

Duman, R.S., 2004. Depression: a case of neuronal life and death? Biol. Psychiatry 56, 140–145.

Ekdahl, C.T., Classen, J.H., Bonde, S., Kokaia, Z., Lindvall, O., 2003. Inflammation is detrimental for neurogenesis in adult brain. Proc. Natl. Acad. Sci. U. S. A. 100, 13632–13637.

Ha, E., Jung, K.H., Choe, B.K., Bae, J.H., Shin, D.H., Yim, S.V., Baik, H.H., 2006. Fluoxetine increases the nitric oxide production via nuclear factor kappa B-mediated pathway in BV2 murine microglial cells. Neurosci. Lett. 397, 185–189.

Hashioka, S., Han, Y.H., Fujii, S., Kato, T., Monji, A., Utsumi, H., Sawada, M., Nakanishi, H., Kanba, S., 2007. Phospholipids modulate superoxide and nitric oxide production by lipopolysaccharide and phorbol 12-myristate-13-acetate-activated microglia. Neurochem. Int. 50, 499–506.

Inazu, M., Takeda, H., Ikoshi, H., Sugisawa, M., Uchida, Y., Matsumiya, T., 2001. Pharmacological characterization and visualization of the glial serotonin transporter. Neurochem. Int. 39, 39–49.

Itagaki, S., McGeer, P.L., Akiyama, H., Zhu, S., Selkoe, D., 1989. Relationship of microglia and astrocytes to amyloid deposits of Alzheimer disease. J. Neuroimmunol. 24, 173–182.

Kanzawa, T., Sawada, M., Kato, M., Yamamoto, K., Mori, H., Tanaka, R., 2000. Differentiated regulation of allo-antigen presentation by different types of murine microglial cell lines. J. Neurosci. Res. 62, 383–388.

Kubera, M., Lin, A.H., Kenis, G., Bosmans, E., van Bockstaele, D., Maes, M., 2001. Anti-inflammatory effects of antidepressants through suppression of the interferon-gamma/interleukin-10 production ratio. J. Clin. Psychopharmacol. 21, 199–206.

Kubera, M., Kenis, G., Bosmans, E., Kajta, M., Basta-Kaim, A., Scharpe, S., Budziszewska, B., Maes, M., 2004. Stimulatory effect of antidepressants on the production of IL-6. Int. Immunopharmacol. 4, 185–192.

Maes, M., Scharpe, S., Meltzer, H.Y., Okayli, G., Bosmans, E., D'Hondt, P., Vanden Bossche, B.V., Cosyns, P., 1994. Increased neopterin and interferon-gamma secretion and lower availability of L-tryptophan in major depression: further evidence for an immune response. Psychiatry Res. 54, 143–160.

Maes, M., Song, C., Lin, A.H., Bonaccorso, S., Kenis, G., De Jongh, R., Bosmans, E., Scharpe, S., 1999. Negative immunoregulatory effects of antidepressants: inhibition of interferon-gamma and stimulation of interleukin-10 secretion. Neuropsychopharmacology 20, 370–379.

Maes, M., Kenis, G., Kubera, M., De Baets, M., Steinbusch, H., Bosmans, E., 2005. The negative immunoregulatory effects of fluoxetine in relation to the cAMP-dependent PKA pathway. Int. Immunopharmacol. 5, 609–618.

Malberg, J.E., Blendy, J.A., 2005. Antidepressant action: to the nucleus and beyond. Trends Pharmacol. Sci. 26, 631–638.

Malberg, J.E., Eisch, A.J., Nestler, E.J., Duman, R.S., 2000. Chronic antidepressant treatment increases neurogenesis in adult hippocampus. J. Neurosci. 20, 9104–9110.

McGeer, P.L., McGeer, E.G., 2004. Inflammation and the degenerative diseases of aging. Ann. N. Y. Acad. Sci. 1035, 104–116.

Merendino, R.A., Mancuso, G., Tomasello, F., Gazzara, D., Cusumano, V., Chillemi, S., Spadaro, P., Mesiti, M., 1994. Effects of lithium carbonate on cytokine production in patients affected by breast cancer. J. Biol. Regul. Homeost. Agents 8, 88–91.

Miller, D.B., O'Callaghan, J.P., 2005. Depression, cytokines, and glial function. Metabolism 54, 33–38.

Miller, D.K., Wong, E.H., Chesnut, M.D., Dwoskin, L.P., 2002. Reboxetine: functional inhibition of monoamine transporters and nicotinic acetylcholine receptors. J. Pharmacol. Exp. Ther. 302, 687–695.

Monje, M.L., Toda, H., Palmer, T.D., 2003. Inflammatory blockade restores adult hippocampal neurogenesis. Science 302, 1760–1765.

Moreno-Lopez, B., Romero-Grimaldi, C., Noval, J.A., Murillo-Carretero, M., Matarredona, E.R., Estrada, C., 2004. Nitric oxide is a physiological inhibitor of neurogenesis in the adult mouse subventricular zone and olfactory bulb. J. Neurosci. 24, 85–95.

Mowla, A., Mosavinasab, M., Pani, A., 2007. Does fluoxetine have any effect on the cognition of patients with mild cognitive impairment?: a double-blind, placebo-controlled, clinical trial. J. Clin. Psychopharmacol. 27, 67–70.

Obuchowicz, E., Kowalski, J., Labuzek, K., Krysiak, R., Pendzich, J., Herman, Z.S., 2006. Amitriptyline and nortriptyline inhibit interleukin-1β release by rat mixed glial and microglial cell cultures. Int. J. Neuropsychopharmacol. 9, 27–35.

Reif, A., Schmitt, A., Fritzen, S., Chourbaji, S., Bartsch, C., Urani, A., Wycislo, M., Mossner, R., Sommer, C., Gass, P., Lesch, K.P., 2004. Differential effect of endothelial nitric oxide synthase (NOS-III) on the regulation of adult neurogenesis and behaviour. Eur. J. Neurosci. 20, 885–895.

Santarelli, L., Saxe, M., Gross, C., Surget, A., Battaglia, F., Dulawa, S., Weisstaub, N., Lee, J., Duman, R., Arancio, O., Belzung, C., Hen, R., 2003. Requirement of hippocampal neurogenesis for the behavioral effects of antidepressants. Science 301, 805–809.

Schiepers, O.J., Wichers, M.C., Maes, M., 2005. Cytokines and major depression. Prog. Neuropsychopharmacol. Biol. Psychiatry 29, 201–217.

Smith, R.S., 1991. The macrophage theory of depression. Med. Hypotheses 35, 298–306.

Steiner, J., Bielau, H., Brisch, R., Danos, P., Ullrich, O., Mawrin, C., Bernstein, H.G., Bogerts, B., in press. Immunological aspects in the neurobiology of suicide: Elevated microglial density in schizophrenia and depression is associated with suicide. J. Psychiatr. Res. doi: 10.1016/j.jpsychires.2006.10.013.

Szuster-Ciesielska, A., Tustanowska-Stachura, A., Slotwinska, M., Marmurowska-Michalowska, H., Kandefer-Szerszen, M., 2003. In vitro immunoregulatory effects of antidepressants in healthy volunteers. Pol. J. Pharmacol. 55, 353–362.

Vallieres, L., Campbell, I.L., Gage, F.H., Sawchenko, P.E., 2002. Reduced hippocampal neurogenesis in adult transgenic mice with chronic astrocytic production of interleukin-6. J. Neurosci. 22, 486–492.

Weinberger, S.B., Schulteis, G., Fernando, A.G., Bakhit, C., Martinez, J.L., 1988. Decreased locomotor activity produced by repeated, but not single, administration of murine-recombinant interferon-gamma in mice. Life Sci. 42, 1085–1090.

Wong, M.L., Whelan, F., Deloukas, P., Whittaker, P., Delgado, M., Cantor, R. M., McCann, S.M., Licinio, J., 2006. Phosphodiesterase genes are associated with susceptibility to major depression and antidepressant treatment response. Proc. Natl. Acad. Sci. U. S. A. 103, 15124–15129.

Xia, Z., DePierre, J.W., Nassberger, L., 1996. Tricyclic antidepressants inhibit IL-6, IL-1 beta and TNF-alpha release in human blood monocytes and IL-2 and interferon-gamma in T cells. Immunopharmacology 34, 27–37.

Yoshimura, A., 2006. Signal transduction of inflammatory cytokines and tumor development. Cancer Sci. 97, 439–447.

Zhu, D.Y., Liu, S.H., Sun, H.S., Lu, Y.M., 2003. Expression of inducible nitric oxide synthase after focal cerebral ischemia stimulates neurogenesis in the adult rodent dentate gyrus. J. Neurosci. 23, 223–229.

Pflugers Arch - Eur J Physiol
DOI 10.1007/s00424-007-0339-7

Early and late activation of the voltage-gated proton channel during lactic acidosis through pH-dependent and -independent mechanisms

Hirokazu Morihata · Junko Kawawaki · Masako Okina · Hiromu Sakai · Takuya Notomi · Makoto Sawada · Miyuki Kuno

Received: 10 June 2007 / Accepted: 27 August 2007

Abstract Voltage-gated proton (H^+) channels play a pivotal role in compensating charge and pH imbalances during respiratory bursts in phagocytes. Lactic acidosis is a clinically important metabolic condition accompanying various tissue disorders in which the extracellular pH and the intracellular pH often change in parallel. In this study, we investigated the responses of the H^+ channel in microglia to lactate-induced pH disturbances using the perforated-patch recordings. Na-lactate (pH 6.8) acidified the cells and activated the H^+ channel within 5 min. This early activation was correlated with increases in the pH gradient across the plasma membrane (ΔpH) and was dose-dependent over a concentration range of 10–150 mM. At 10 mM, the change in ΔpH was only slight, but the H^+ currents continued to increase over an hour after the cell acidosis was stabilized. Prolonged exposure to lactate (10–20 mM, >1 h) increased the amplitude by two to threefold. The late activation was not explained by increased ΔpH but by changes in the property of the channel per se. Pretreatment with staurosporine and chelerythrine, inhibitors for protein kinase C, prevented the late activation. These results suggest that the H^+ channel could be activated greatly during long-lasting lactic acidosis through both ΔpH-dependent and -independent mechanisms.

Keywords Proton current · Lactic acid · Acidosis · Protein kinase C · pH

H. Morihata M. Okina H. Sakai T. Notomi M. Kuno (✉)
Department of Physiology,
Osaka City University Graduate School of Medicine,
Abeno-ku, Osaka 545-8585, Japan
e-mail: kunomyk@med.osaka-cu.ac.jp

J. Kawawaki
Central Laboratory,
Osaka City University Graduate School of Medicine,
Osaka 545-8585, Japan

M. Sawada
Department of Brain Life Science,
Research Institute of Environmental Medicine,
Nagoya University,
Nagoya 464-8601, Japan

M. Kuno
Department of Molecular Physiology, Division of Intracellular Metabolism, National Institutes of Natural Sciences,
Okazaki 444-8585, Japan

Introduction

Voltage-gated proton (H^+) channels, first described in snail neurons [33], are characterized by extremely high selectivity for H^+ and large H^+ effluxes [1]. They play a pivotal role in the respiratory bursts during phagocytosis [5, 12, 23]. It is deduced, from the electrophysiological properties, that the H^+ channels respond to changes in both extracellular pH (pH_o) and intracellular pH (pH_i). The activation thresholds and the driving forces for H^+ efflux through the channel are determined primarily by the pH gradient across the plasma membrane ($\Delta pH = pH_o - pH_i$). Thus, the effects of pH_i and pH_o on the voltage dependence are reciprocal: H^+ channels are activated at more positive voltages by decreases in pH_o, but at more negative voltages by decreases in pH_i. Pathological conditions, such as hypoxia, ischemia, injury and degenerating diseases, are accompanied by a disturbance of the pH homeostasis: pH_i and pH_o often change in parallel and interfere mutually. Therefore, tissue acidosis may increase or decrease ΔpH. Lactic acidosis is a clinically important metabolic acidosis and fits this case [10, 22, 29, 32].

The lactic acid generated by anaerobic glycolysis may accumulate in tissue. Lactate-induced extracellular acidification stimulates H^+-sensing channels such as the acid-sensing Na^+ channels (ASIC) [14]. The behavior of H^+ channels might, however, be more complicated. If pH_i is decreased more than pH_o, the channel would be activated. In contrast, the channel must be inhibited when the drop of pH_i is smaller than that of pH_o. Our previous study showed that a high concentration (150 mM) of lactate increased ΔpH [22], but the concentration was too high to generalize the results to the case of moderate lactic acidosis. Therefore, the dose-dependent effect of lactate on the ΔpH should be evaluated. In addition, lactic acid induces a variety of cellular responses, for instance, mitochondrial dysfunction, cell swelling, and production of free radicals, leading to deleterious effects on cellular functions [2, 10, 17, 22, 25, 32]. Besides the direct effects of ΔpH, the subsequent biological actions could affect the channel activity. To resolve these issues, it is essential to measure the H^+ channel currents from the cells exposed to lactic acidosis. However, the lactate-mediated cell acidosis could not be introduced under the whole-cell clamp configuration in which pH_i is controlled by the pipette solution. In addition, modulation of the H^+ channel activity through second messenger pathways, such as activation by protein kinase C [4], was often hampered by the intracellular dialysis.

This study focused on investigating the dose- and time-dependent behavior of the H^+ channel under lactic acidosis using the perforated-patch recordings in microglia which expresses the H^+ channel consistently [6, 7, 21, 22]. The perforated-patch recordings appear to be most suitable for minimizing perturbation of the intracellular environment and preserving cellular buffer actions. Electrophysiological analyses permitted the estimation of cell acidosis and ΔpH-dependent events. The data suggested that the H^+ channel would be activated during lactic acidosis through ΔpH-dependent and -independent mechanisms.

Materials and methods

Cells A rat microglial cell line (GMI-R1) [28] was cultured in the Eagle's MEM containing 1 ng/ml recombinant mouse GM-CSF (Peprotec), 10 ng/ml insulin, 10 mM glucose, 100 U/ml penicillin, 0.1 mg/ml streptomycin, 0.25 ng/ml amphotericin B, and 10% fetal calf serum. Cells were plated at a density of $1.0–2.0 \times 10^5$ cells/ml on coverslips and were incubated at 37°C in a 95% air–5% CO_2 atmosphere. The culture medium was changed every 3–4 days. GMI-R1 cells preserve microglial characteristics [28] and exhibit H^+ channels consistently [21]. The properties of the H^+ channels share the same characteristics with those in microglia in primary culture [6, 7, 21, 22].

Solutions The standard Ringer solution contained (in millimolar): 145 NaCl, 5 KCl, 1 $CaCl_2$, 1 $MgCl_2$, and 10 HEPES (pH 7.3). The Na^+-free K^+-rich solution and the $NMDG^+$ solution were made by replacing NaCl with either KCl or *N*-methyl-D-glucamine (NMDG) chloride. To load cells with NH_4^+, NaCl was replaced by 40 mM NH_4Cl. Na-lactate solutions were made with 10–150 mM Na-lactate, 0 or 5 mM KCl, 1 mM $CaCl_2$, 1 mM $MgCl_2$, 10 mM Hepes (pH 6.8). The osmolarities were adjusted by adding either Na-isethionate or NaCl. There was no consistent difference in the results between the solutions containing Na-isethionate and NaCl. All solutions were supplemented with 10 mM glucose and 0.1% bovine serum albumin (BSA). The osmolarities of the solutions were measured using a freezing-point depression osmometer (OS osmometer, Fiske, MA, USA) and were maintained between 285 and 300 mosmol/l.

Electrophysiological recordings In perforated-patch recordings, the standard pipette solutions contained: 150 mM Cs-methansulfonate, 3 mM $MgCl_2$, 1 mM EGTA, 10 mM Hepes, and amphotericin B (500 μg/ml; pH 7.3). The standard extracellular solution was 150 mM Na-isethionate, 1 mM $CaCl_2$, 1 mM $MgCl_2$, 10 mM Hepes, 10 mM glucose, and 0.1% BSA (pH 7.3). As the microglia express K^+ channels, K^+ was generally omitted from both intracellular and extracellular solutions. The K^+ concentration (0–5 mM) did not affect the results in voltage-clamped cells in which the holding potential was maintained. In most of recordings, 50 μM 4,4′-diisothiocyano-2,2′-stilbenedisulfonic acid (DIDS), a Cl^- channel blocker, was added to the bath solution. The buffer molecules (Hepes) could not pass through the amphotericin B pores [20], and so the pH_i was controlled by the intrinsic pH buffers. The membrane potential was measured under the current-clamp configuration in the standard Ringer solution: Cs-methanesulfonate in the pipette solution was replaced by K-gluconate. To characterize the electrophysiological properties of the channel per se, H^+ currents were recorded in whole-cell recordings. Major ions (Na^+, K^+ and Cl^-) were removed from both bath and pipette solutions. The pipette contained 65 mM NMDG-aspartate, 3 mM $MgCl_2$, 1 mM BAPTA, 120 mM Mes (pH 5.5–6.5). The pH was adjusted by CsOH or KOH. The bath contained (in millimolar): 75 NMDG-aspartate, 100 Hepes, 1 $MgCl_2$, 1 $CaCl_2$ and 50 μM DIDS (pH 7.3). Ten millimolar glucose and 0.1% BSA were added into the bath solutions. The osmolarities of the solutions were maintained between 280 and 290 mosmol/l.

The reference electrode was a Ag–AgCl wire connected to the bath solution through a Ringer-agar bridge. The liquid junction potential was corrected before formation of the gigaseal in all experiments. The pipette resistances ranged between 5 and 15 MΩ. Current or voltage signals

were recorded with an amplifier (Axopatch 200A, Axon Instruments, Foster City, CA, USA), digitized at 2 kHz with an analog-digital converter (Digidata 1200, Axon Instruments), and analyzed using pCLAMP software (Axon Instruments). Proton currents were evoked by depolarization pulses (1–4 s) applied at the holding potentials (−80–0 mV) every 10–20 s. Leak currents were estimated from the linear portion of the current-voltage (*I–V*) relation at voltages lower than the threshold potential for the H^+ channel. The leak currents were subtracted from the current records. All experiments were carried out at room temperature (22–24°C) [18].

Data analysis The activation process was fitted with a single exponential function after a delay time, giving estimates of the steady-state currents and the activation time constants (τ_{act}). The reversal potentials (V_{rev}) were obtained by either the tail-current method or the repolarization-pulse method [11, 18, 20]. In the former, the *I–V* relationships were obtained from instantaneous tail currents at different voltages following a constant voltage pulse (+100 mV, 1–2 s). In the latter, the *I–V* relationships were obtained by applying 20-ms-long repolarization voltage-ramps at the end of 2-s-long depolarization (40–100 mV). Subtraction of the leak and capacitive currents after a short (20 ms) depolarization yielded the net *I–V* curves for the H^+ currents. The V_{rev}s were obtained from the zero-current voltages. In the perforated-patch recordings, the tail current method was used, as the higher access resistance might generate voltage error during the short repolarization voltage-ramp. Data are means±SEM. The statistical significances ($p<0.05$) were evaluated using Student's unpaired *t* test, unless described otherwise.

We used the cell diameter ratios to monitor cell swelling, as the increases in the cell diameters were almost proportional to the estimates using the dye-dilution method or the measurements of the cell thicknesses during swelling [22].

Measurements of intracellular pH (pH_i) The intracellular pHs (pH_i) of single cells were determined with a digital fluorescence microscopy (Attoflour, Zeiss) using a pH-sensitive fluorescent dye, 2′,7′-bis-(2-carboxyethyl)-5 (and -6) carboxyfluorescein (BCECF). Cells were plated on glass coverslips for 10–24 h and loaded with the acetoxymethyl ester form of BCECF (BCECF-AM; 1 μM) for 30 min at 37°C. After washout of the dye, the ratios of the fluorescence images (the emission wavelength ≥520 nm) excited at two wavelengths (488 and 460 nm) were measured every 10 s with 30- to 100-ms exposures. Data (80–120 pixels for each cell) for each illumination were averaged and plotted against time. Calibration of pH_i was carried out by dissipating ΔpH with 10 μM nigericin in a K^+-rich solution with known pH values [9].

TUNEL staining Apoptotic effects of PKC inhibitors were examined with the method of TdT-mediated dUTP-biotin nick end labeling (TUNEL). Briefly, cells were fixed in 4% paraformaldehyde, permeabilized in 0.1% TritonX-100/0.1% sodium citrate, and stained with fluorescein-labeled TUNEL reaction mixture (Roche). Analysis by fluorescence microscopy revealed that TUNEL-positive cells were none at 2-h treatment with 100 nM staurosporine and 2–3% at 6 h.

Substances MES, BAPTA, and BCECF-AM were purchased from Dojindo Laboratories (Kumamoto, Japan), and all other chemicals were obtained from Sigma Chemical Co. (St. Louis, MO, USA). Concentrated stock solutions of DIDS, staurosporine, and chelerythrine chloride were prepared in DMSO and that of nigericin in ethanol. The final concentrations of DMSO and ethanol were less than 0.1 and 1%, respectively, which affected neither the currents nor the cell shapes.

Results

Activation of the voltage-gated proton channel in response to cell acidosis

The whole-cell H^+ currents in microglia were characterized as slowly activating outward currents evoked by depolarization (Fig. 1a) [7, 21, 22]. As the cell inside was dialyzed continuously with the pipette solution, pH_i was determined

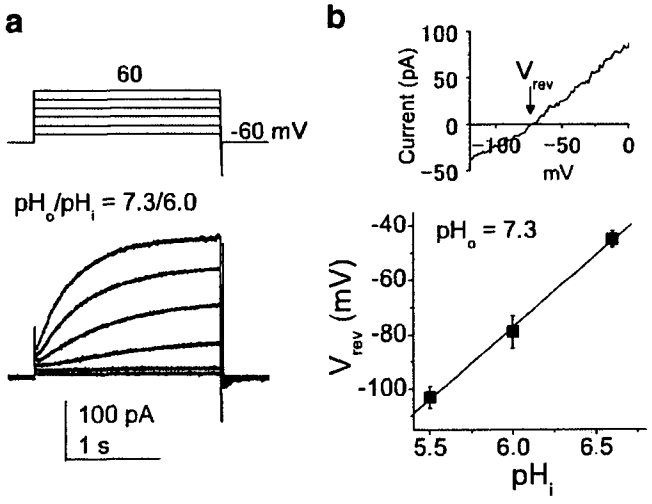

Fig. 1 The pH dependence of the H^+ channel. a Representative whole cell H^+ currents evoked by depolarization pulses applied at −60 mV. pH_o/pH_i = 7.3/6.0. Leak currents were not subtracted. In later figures, the leak currents were subtracted from the current records. b The V_{rev} was obtained from the zero-current voltages of the net I–V curve (*arrow* in inset). V_{rev}s were plotted against pH_i of 5.5 (n=21), 6.0 (n=4), and 6.5 (n=5) at a constant pH_o (7.3). The relationship was linear with a slope of 53 mV/unit pH_o. Data are means±SEM

by the pH of the pipette solutions. The reversal potentials (V_{rev}) were obtained from the net *I–V* relation using the repolarization-pulse method (Fig. 1b, inset; see "Materials and methods"). The V_{rev} was determined by the pH gradient across the plasma membrane ($\Delta pH = pH_o - pH_i$), as the H^+ channel is highly selective for H^+. At a constant pH_o (7.3), V_{rev} was correlated with pH_i (Fig. 1b). The whole-cell clamp configuration stabilizes the pH_o and pH_i with high concentrations of pH buffers, which does not permit changes in the pH environment in response to various cellular conditions. In the perforated-patch recordings, pH_i could not be set with the pH buffers (Hepes or Mes) in the pipette solution, as the buffers did not pass through amphotericin B pores. Changes in pH_i and the channel activity could be investigated under the action of cellular buffers. However, the pH of the pipette solution (pH_p) was maintained to be constant (7.3) throughout the experiments, which might affect in pH_i. To confirm whether intracellular acidosis could be induced under this recording condition, first, we examined the behavior of the H^+ channel in response to purely intracellular acidification at constant pH_o.

Figure 2a shows averaged change of pH_i, monitored by a pH-sensitive fluorescent dye (BCECF), in cells exposed to 40 mM NH_4Cl. The pH_o was set to 7.3 throughout the experiment. The resting pH_i of single microglia was 7.32± 0.02 (n=70) in the standard Ringer solution. The pH_i was elevated transiently by application of NH_4Cl. Washout of NH_4Cl decreased pH_i rapidly, but the intracellular acidification was recovered in the Na^+-free, K^+-rich solution, which depolarized microglia (−5±5 mV, n=5). In cells incubated with 40 mM NH_4Cl for 30 min, the pH_i was 7.27±0.03 (n=52). Washout of NH_4Cl with the K^+-rich solution decreased pH_i by ~1.0 U (Fig. 2b, upper closed circle) and then returned the pH_i towards the pre-wash level. Perforated-patch recordings revealed that the H^+ channel was activated during this acutely induced cell acidosis

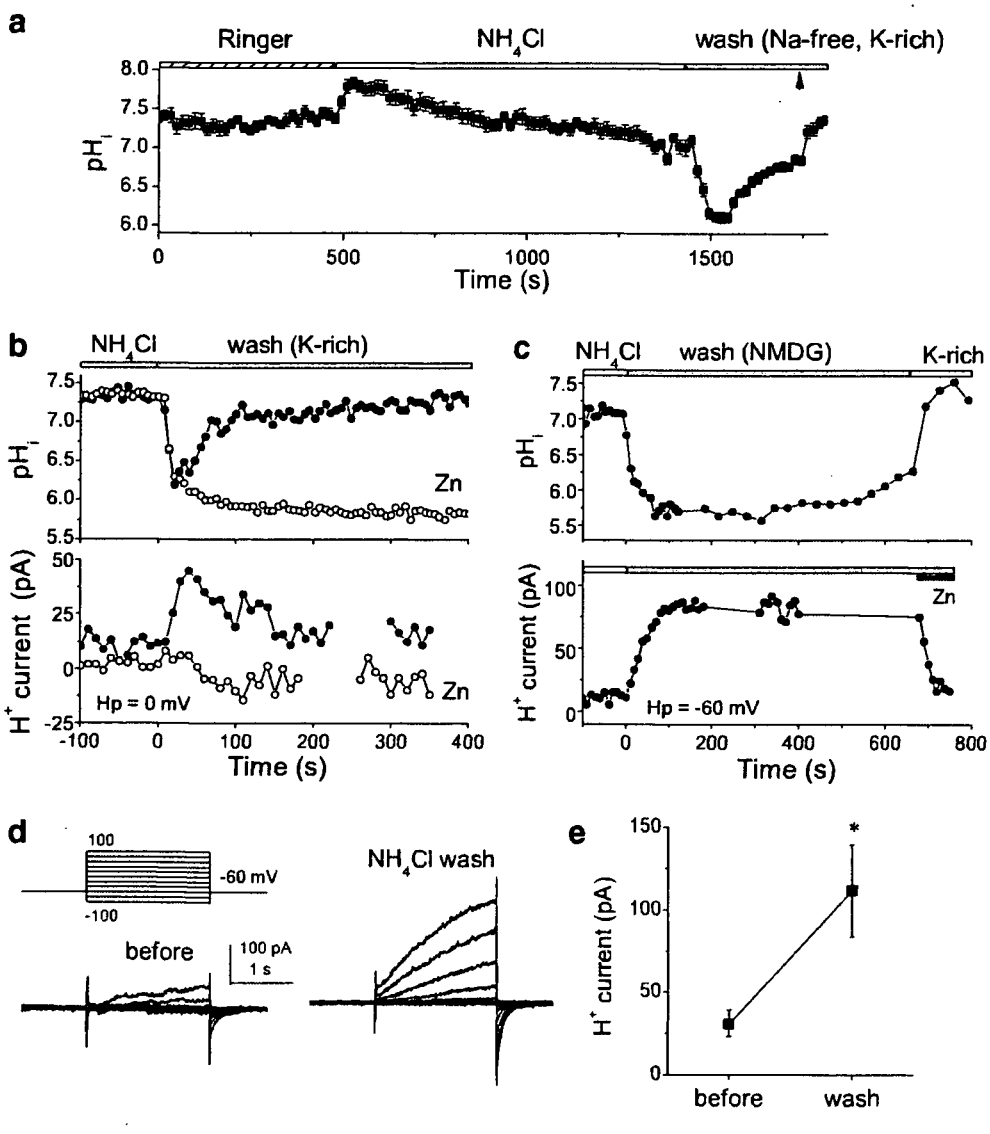

Fig. 2 Acute cell acidosis and H^+ channel activation induced by washout of pre-loaded NH_4Cl. **a** An averaged time course of changes in pH_i measured with BCECF from 15 cells exposed to 40 mM NH_4Cl. The cells were washed with a Na^+-free K^+-rich solution which depolarized the cell. Finally, nigericin was added (*arrowhead*) for calibration. pH_o was 7.3. **b** The pH_i recovery in a single cell exposed to 40 mM NH_4Cl for 30 min (*upper*). *Open symbols* represent data in the presence of 100 μM $ZnCl_2$. The H^+ current amplitudes (*lower*) were the responses evoked by a 1-s-long depolarization (−100 mV) pulse every 10 s applied at a holding potential of 0 mV. **c** pH_i responses (*upper*) and H^+ channel activation (*lower*) in hyperpolarized microglia. *Upper* NH_4Cl was replaced by a $NMDG^+$-rich solution. *Lower* The holding potential was kept at −60 mV. **d** H^+ currents evoked by step pulses applied at −60 mV in a perforated-patch before and at 3 min after washout of 40 mM NH_4Cl. **e** Mean H^+ current amplitudes measured at the end of depolarization pulse (100 mV, 2 s) before and after washout of NH_4Cl (n=9). Data are means± SEM. *p<0.05 (paired t test)

(Fig. 2b, lower closed circle). The membrane potential was held to 0 mV, except for a test pulse (100 mV, 1 s) applied every 10 s. The time course of the change in the H^+ current was similar to that in pH_i: the H^+ currents increased with the drop in pH_i and then declined along with the recovery of pH_i. The time constant of the pH_i recovery was 128±8 s (n=25), not significantly different from that for the decrease in the H^+ currents (112±13 s, n=5). Zinc, a blocker for the H^+ channel, inhibited both the pH_i recovery and the current activation (Fig. 2b, open circles), indicating that the H^+ channel contributed to the quick relief of cell acidosis in depolarized cells.

When cells were hyperpolarized by the $NMDG^+$ solution (−75±12 mV, n=3), the cell acidosis following washout of NH_4Cl was maintained until the cells were depolarized by the K^+-rich solution (Fig. 2c, upper). The H^+ channel continued to be activated in cells maintained at a holding potential of −60 mV (lower). Thus, changes in pH_i and H^+ channel activation were highly correlated: activation of the H^+ channel started by a drop in pH_i, lasted as far as the cell acidosis was maintained and terminated with the relief of the cell acidosis. Washout of NH_4Cl increased the amplitudes of the H^+ currents recorded in the perforated-patch configuration at all potentials tested (Fig. 2d), by two to fivefold (Fig. 2e). These observations showed that the present recording condition was suitable for investigating the H^+ channel activity under cell acidosis.

Lactate induces intracellular acidification and activation of the H^+ channel

We next investigated the response of the H^+ channel to lactic acidosis at a pH_o set at 6.8. The Na-lactate solutions generated sustained cell acidosis in microglia (Fig. 3a) [22]. The pH_i fell within 2–3 min to ~6.7 for 10 mM lactate, ~6.5 for 20 mM lactate and ~6.0 for 150 mM lactate. Thus, both pH_o and pH_i decreased during lactic acidosis. The subtraction gave changes in ΔpH (Fig. 3b). Lactate increased ΔpH (at 5 min) dose-dependently over 10–150 mM (Fig. 3c). The pH_i and ΔpH recovered rapidly after depolarizing the cells with the K^+-rich solution (pH 7.3; Fig. 3a and b).

The H^+ currents were increased within a few minutes after application of Na-lactate (Fig. 4a). At higher lactate concentrations, the activation was faster and more marked. Lactate increased the amplitude of the current and also facilitated the activation process upon depolarization at all potential tested (Fig. 4b); these effects were similar to the responses produced by washout of NH_4Cl. The data were fitted with a single exponential function, giving estimates of the steady-state currents and τ_{act}. The increases in the amplitudes of the steady-state currents and the decreases in τ_{act} produced by 5-min exposure of Na-lactate were dose-dependent (Fig. 4c). Lactate (150 mM) increased the current amplitudes by three to fourfold of the control and decreased the τ_{act} to one third.

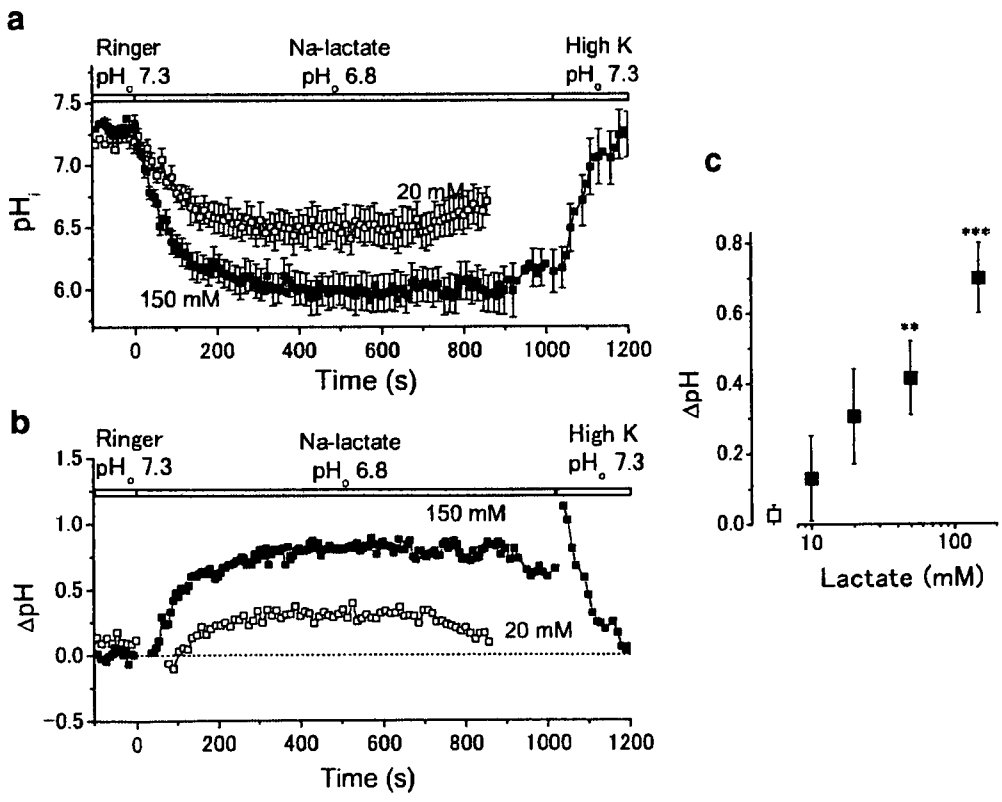

Fig. 3 pH Responses during lactic acidosis. **a** Time courses of the pH_i changes in the presence of 20 mM (*open squares*, n=8) and 150 mM Na-lactate (*closed squares*, n=7). pH_o of lactate solutions was 6.8. Washout by the Na^+-free K^+-rich solution increased pH_i quickly. **b** Time courses of the changes in ΔpH ($pH_o - pH_i$) for the data in **a**. **c** The dose-response relationship for ΔpH at the steady-state (5–10 min). Data are 0.03±0.03 pH unit (n=52) for control, 0.13±0.12 (n=17) for 10 mM, 0.31±0.13 (n=8) for 20 mM, 0.42±0.11 (n=8) for 50 mM, and 0.70±0.10 (n=15) for 150 mM. Data are means± SEM. $^{**}p<0.005$. $^{***}p<0.0005$

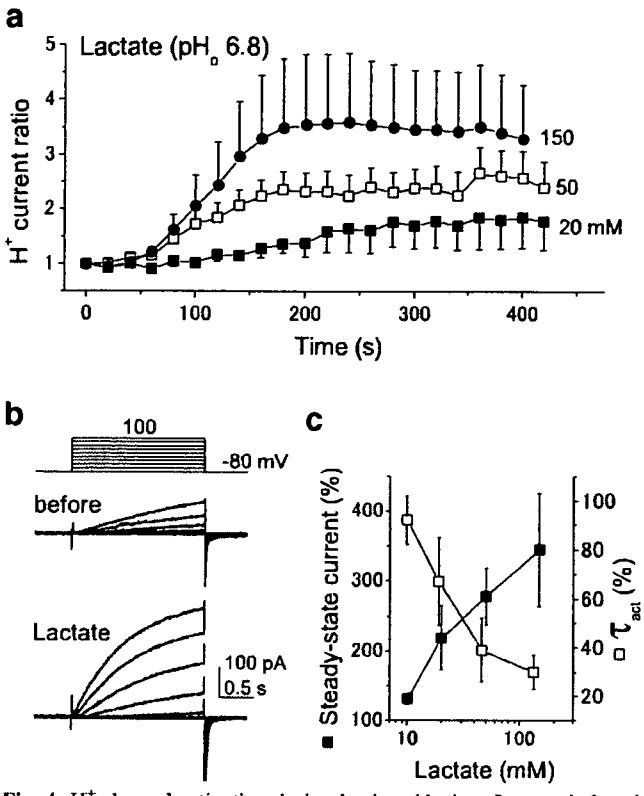

Fig. 4 H^+ channel activation during lactic acidosis. a Lactate-induced activation of H^+ currents under perforated-patch recordings: 20 mM (n=4–5), 50 mM (n=3–6) and 150 mM lactate (n=5). The membrane potential was −80 mV, and the H^+ current was evoked by 1-s-long depolarization (−100 mV) pulse every 20 s. The current ratio was obtained from the relative current magnitudes to those before each exposure to lactate. b H^+ currents before and 5 min after exposure to 50 mM Na-lactate. c The steady-state current amplitudes (*closed squares*) and the activation time constants (τ_{act}; *open squares*) at 5-min exposure to 10–150 mM Na-lactate. Data (mean±SEM) were obtained from the currents evoked by 80–100 mV depolarizations and expressed as percent of the control. Steady-state currents: 130±10% (n=8) for 10 mM, 220±50% (n=7) for 20 mM, 280±40% (n=6) for 50 mM, and 340±80% (n=15) for 150 mM. τ_{act}: 92±10% (n=6) for 10 mM, 67±18% (n=3) for 20 mM, 39±13% (n=3) for 50 mM and 30±7% (n=7) for 150 mM. Data are means±SEM

The *I–V* relationships of cells during the acidosis induced by washing of NH_4Cl (Fig. 5a, left) or by a 5-min exposure to 50 mM lactate (Fig. 5c, left) were shifted towards more negative potentials. The V_{rev} measured using the tail-current method is indicated by arrowhead. The V_{rev} was shifted in negative direction by lactate. The shift of ΔpH was calculated from the V_{rev} shift (ΔV_{rev}) using the linear relationship between V_{rev} and ΔpH (Fig. 1b). The ΔpH shift after NH_4Cl washout was ~0.8–0.9 U (Fig. 5b). The estimated ΔpH shift by lactate was increased dose-dependently (Fig. 5d). As the pH_o was decreased by 0.5 U, from 7.3 to 6.8, the pH_i drop could be evaluated by adding 0.5 U to the ΔpH shift. For example, the increase in ΔpH by 0.8 U at 150 mM means that the pH_i was reduced by approximately −1.3 U.

Progressive activation of the H^+ channel during prolonged lactic acidosis

As described above, an increase in ΔpH, the driving force for H^+ efflux, is a common mechanism to enhance the H^+ currents during cell acidosis induced by either washout of preloaded NH_4Cl or by application of Na-lactate. When the *I–V* curve obtained after the washout of NH_4Cl was moved positively to cancel the V_{rev} shift, the two *I–V* curves overlapped well (Fig. 5a, right). In this case, it is likely that the H^+ currents were enhanced mainly by the increase in the driving force for H^+. However, the two *I–V* curves, before and after stimulation with lactate, did not overlap (Fig. 5c right). The amplitudes of the currents at the same driving force were greater in the presence of lactate than those in the controls, suggesting that mechanisms other than increases in ΔpH may be involved in the lactate-induced activation of the H^+ channel. Prolonged exposure to lower concentrations (≤20 mM) of lactate revealed clearly that lactate activated the H^+ channel more strongly than expected from the ΔpH change itself: stable intracellular acidosis was attained within 5 min (Fig. 3a), but the H^+ currents continued to increase (Fig. 6a–c). Figure 6a shows a time course of progressive activation of the H^+ current with 10 mM lactate. The current reached the steady-state after 1 h. Although the increase in ΔpH by 10 mM lactate was only slight (Fig. 5d), the exposure for >1 h increased the current amplitude by approximately twofold (Fig. 6a–c). With 20 mM lactate, the current amplitude at >1 h was increased by approximately threefold (Fig. 6c), which was almost equal to the amount attained by 5-min exposure of 150 mM lactate.

To confirm the ΔpH-independent activation more clearly, whole-cell recordings were made in cells incubated with 20 mM lactate for >1 h. To stabilize ΔpH, pH_o and pH_i were set to be 7.3 and 5.5 with high concentrations (100–120 mM) of pH buffers. At a constant driving force, lactate enhanced the steady-state current amplitude by approximately twofold (Fig. 6d, left) and decreased τ_{act} to half (right). These results showed that properties of the H^+ channel per se were modulated so as to increase the H^+ current during long-lasting lactic acidosis.

PKC inhibitors prevent the late activation of the H^+ channel

Protein kinase C (PKC) is a strong activator for the H^+ channel [4, 20, 24]. Figure 7 summarizes the lactate (10 mM)-induced changes when the cells were preincubated with PKC inhibitors, staurosporine and chelerythrine. Both staurosporine (100 nM, >2 h) and chelerythrine (2 μM, >1 h) prevented the late increase in the amplitude of the steady-state current (a) and the lactate-induced decrease in τ_{act}. The

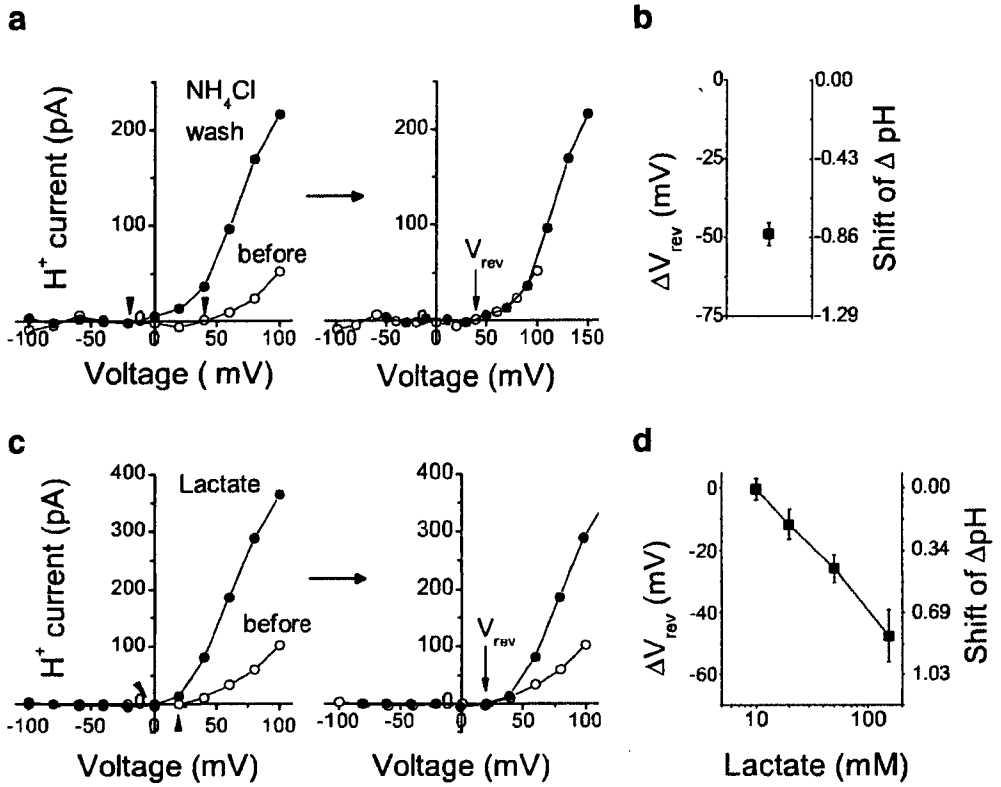

Fig. 5 Current–voltage (*I–V*) relationships and the reversal potentials (V_{rev}) of the H^+ channel during cell acidosis in the perforated-patch recordings. **a** *Left*, *I–V* plots for the steady-state current before (*open circles*) and after washout of pre-loaded NH_4Cl (*closed circles*). *Arrowheads* indicate V_{rev} estimated by the tail-current method (see "Materials and methods"). The two *I–V* curves were superimposed by moving the control curve to cancel the difference in the two V_{rev}s (*right*, *arrow*). **b** The shift of V_{rev} (ΔV_{rev}): −49±4 mV (n=4). The corresponding shift of ΔpH (0.84±0.06 pH unit, n=4) is indicated on the *right*. pH_o was maintained at 7.3 throughout the experiments. **c** *Left*, *I–V* relationships before (*open circles*) and after 5-min exposure to 50 mM Na-lactate (*closed circles*). *Right*, the *I–V* curve upon lactic acidosis was moved towards positive potentials to cancel the difference in the two V_{rev}s: **d** The shift of V_{rev} at 5-min exposure to lactate: −0.4±3.5 mV (n=6) for 10 mM, −12±5 mV (n=5) for 20 mM, −26±5 mV (n=6) for 50 mM, and −48±9 mV (n=6) for 150 mM corresponding to the shifts of ΔpH of 0.01±0.06, 0.20±0.08, 0.45±0.08, and 0.82±0.15 pH unit, respectively (on the right scale). pH_o was 7.3 in control and 6.8 in the presence of lactate. Data are means±SEM

inhibitory effects were more prominent at 1 h than those at 5 min The pretreatment with staurosporine or chelerythrine did not affect the H^+ current in the resting state.

Cell swellings and depolarization during prolonged lactic acidosis

Cell swelling is a potent activator for the H^+ channels in microglia [22]. In non-clamped cells, a 10-min exposure to 50 mM Na-lactate increased the cell diameter by ~10% (n=18–23). With 10–20 mM lactate, swelling developed more slowly: The diameter increased by 6.2±2.6% (n=10) with 10 mM and 8.9±2.7% (n=9) with 20 mM at 1 h. This level was maintained for several hours. Staurosporine did not prevent the cell swelling: 10 mM lactate increased the diameter by 6.7±4.1% (n=9) at 1 h even in cells treated with staurosporine (100 nM, 2 h).

The membrane potential recorded in the standard Ringer solution with K^+-containing pipette solution was −50± 10 mV (n=9) in control. There was no consistent change in the membrane potential after 5-min exposure to 20 mM lactate (−45±12 mV, n=8). However, the presence of 20 mM lactate for >1 h depolarized cells to about −10 mV (−12±5 mV, n=8) probably through metabolic disturbances. The depolarization might facilitate the channel openings.

Discussion

The H^+ channel is the most potent H^+-secreting mechanism among various transmembrane H^+ conduction pathways. Understanding the activation mechanisms is crucial in resolving the functional roles of the H^+ channel. The present study revealed that the H^+ channel was activated remarkably during lactic acidosis. The activation process was separated into two phases; an early enhancement due to increases in ΔpH and a later progressive potentiation through changes in properties of the channel per se.

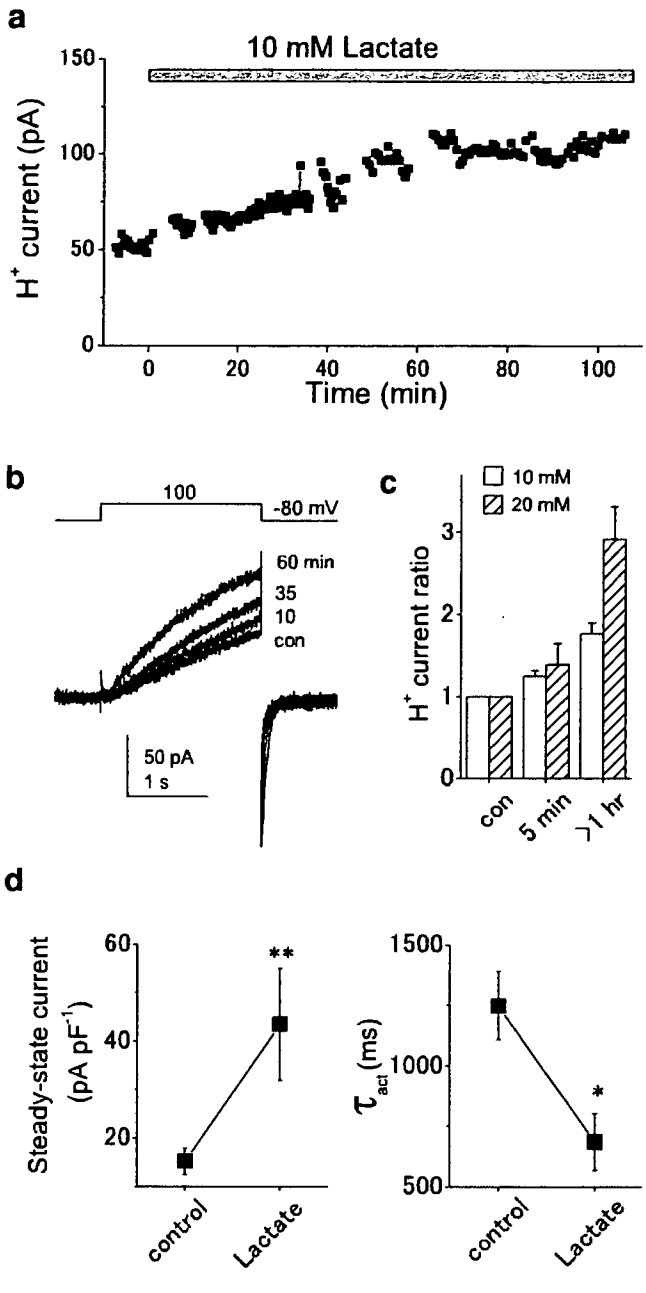

Fig. 6 Progressive activation of the H^+ channel during prolonged lactic acidosis. **a** A time course of gradual increases in H^+ currents in the presence of 10 mM lactate (pH 6.8). **b** H^+ currents (100 mV) recorded in a cell exposed to 10 mM lactate for 10, 35, and 60 min. **c** Relative H^+ current amplitude in cells after incubation with lactate for 5 min (n=4 for 10 mM, n=9 for 20 mM) and >1 h (n=4 for 10 mM, n=11 for 20 mM). The current amplitudes were measured at the end of 2- to 4-s-long depolarization pulses (80–100 mV) applied at −80 mV. **a–c** Obtained from perforated-patch recordings. **d** Whole-cell H^+ currents in control (n=5) and in cells incubated with 20 mM lactate (pH 6.8) for >1 h (n=13). pH_p/pH_o=5.5/7.3. Steady-state current-densities (*left*) and activation time constants (τ_{act}; *right*) were obtained from the responses evoked by depolarization pulses (40 mV) applied at −80 mV. The steady-state current and τ_{act} were 15.2±2.8 pA/pF, 1,250±140 ms for control, 43.5±11.6 pA/pF and 690±120 ms for the treated cells. Data are means±SEM. *p<0.05, **p<0.005

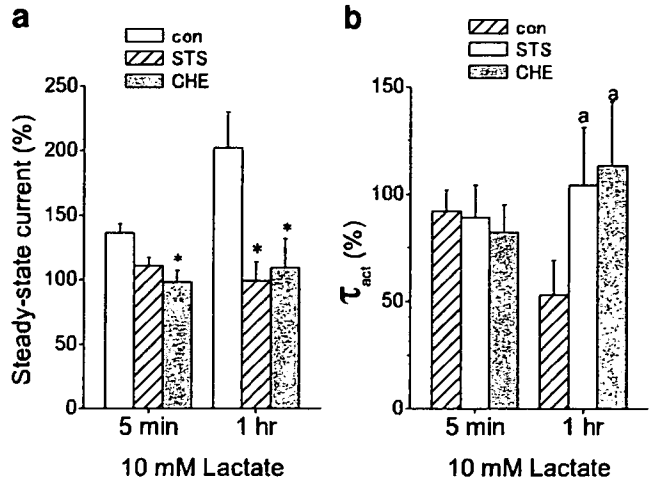

Fig. 7 Effects of PKC inhibitors on the lactate-induced activation of the H^+ current. Relative changes in the steady-state current amplitude (**a**) and τ_{act} (**b**) at 5-min and 1-h exposure to 10 mM lactate (pH 6.8). The data were obtained from the currents evoked by depolarization pulses to −100 mV. The holding potential was −80 mV. The data in cells incubated with 100 nM staurosporine for >2 h (n=3–6) or 2 μM chelerythrine for >1 h (n=4–7) were compared with those in untreated cells (n=4–8). *p<0.05. *a* indicates p=0.2

Cell acidosis introduced in the perforate-patch configuration The electrophysiological features of H^+ channels, well-characterized in the whole-cell condition, show that the activity of H^+ channels is regulated primarily by changes in ambient pH. Therefore, H^+ channels could function as pH sensors. However, the pH-monitoring actions of H^+ channels are distinct from those of acid-sensing channels like vanilloid receptors and ASIC in several features including voltage gating and absence of threshold pH. Moreover, the responsiveness to both pH_i and pH_o complicates the actions of H^+ channels. Purely extracellular acidification decreases the channel activity, but purely intracellular acidification enhances it. However, these conditions seldom occur. Rather, changes in pH_o and pH_i are inseparable and often change in parallel in tissue acidosis. In this study, we employed the perforated-patch recordings to examine the lactate-induced changes in ΔpH and the H^+ channel activity over a wide range of the concentration.

The whole-cell recordings are generally performed under a strict control of pH_i with very high concentrations (100–120 mM) of pH buffers. It has been questioned whether the H^+ channel could respond to pH disturbances as expected even with intrinsic intracellular buffers under the perforated-patch configuration. We checked the fidelity of the recording system from the responses by washout of preloaded NH_4Cl. This is a common experimental procedure to examine the effects of acid-load [13]: cell acidosis can be imposed without changes in pH_o. During the acute cell acidosis, activation of the channel started upon a drop

in intracellular pH and terminated at relief of the cell acidosis. The activation lasted as long as the cell acidosis was sustained. The channel behavior in the acutely induced cell acidosis was well explained by changes in the driving force for H^+: the H^+ current was potentiated by the increase of ΔpH which shifted the activation threshold to more negative voltages and increased the driving force for H^+.

An additional concern of the perforated-patch recordings was whether the constant pH of the pipette solution (pH_p 7.3) might affect introduction of cell acidosis by lactate. The present study showed that cell acidosis was maintained under the perforated-patch configuration as far as lactate was present. At closer inspection, however, the 10 mM lactate-induced shift of ΔpH estimated from the V_{rev} was smaller (~0.01 pH unit; Fig. 5d) than the value obtained by the measurement using BCECF in non-clamped cells (~0.1 pH unit; Fig. 3c). Thus, a small amount of cell acidification may be underestimated under the effect of the pH_p. In addition, the control pH_i calculated from the V_{rev} (17±4 mV, n=8) was ~7.6, higher than the resting pH_i estimated with BCECF in non-clamped cells (~7.3). Proton efflux during the tail current method might increase pH_i, as depletion of protonated buffers shifts the V_{rev} towards more positive voltages even in the whole-cell configuration under high concentrations of pH buffers [3]. Otherwise, absence of Cl^- in the electrophysiological recordings may be responsible for the difference at least partly [26]. In spite of these small variations, the lactate-induced shift of the ΔpH estimated by the two methods was not far different. It is thus likely that the pH responses in the presence of intrinsic intracellular buffers were almost preserved under the present recording conditions.

Lactic acidosis and H^+ channel activation During lactic acidosis, both pH_o and pH_i decreased simultaneously. According to the ΔpH dependence of the channel activity as described above, the activation may occur only when the intracellular acidification exceeds the extracellular acidification. The resultant increase in ΔpH and activation of the H^+ channel were both dose-dependent at 5-min exposure to lactate. The increase in driving force for H^+ seems to be responsible for this early activation.

The increased ΔpH was, however, not enough to explain all the responses produced by lactate. First, the temporal patterns of the changes in ΔpH and the channel activation were not consistent. The current amplitude continued to increase over >1 h, although the pH_i reached the steady-state within 5 min. Second, the increases in the H^+ currents were much greater than those predicted from the increase in the driving force. Therefore, additional mechanisms other than the increase in ΔpH appear to contribute to lactate-induced activation of the H^+ channel, particularly when the exposure to lactate is prolonged. Whole-cell recordings, which could clamp ΔpH with high pH buffers, confirmed the change in the electrophysiological properties of the H^+ channel. The concentration of lactate in the tissue would be less than 10–20 mM. The ΔpH-independent late activation may be more significant in pathological context.

Mechanisms for the late activation by lactate The mechanisms responsible for the ΔpH-independent activation have not yet been fully resolved, but there are several possibilities. Cell acidosis could affect various cellular processes, besides direct effects on ion channels or enzymes: It changes the fluidity of the plasma membrane [15], increases the level of strong free radicals [30], and modifies the cytoarchitecture [8]. Activation of PKC is a mechanism underlying cellular responses in tissue acidosis [16, 19, 27]. H^+ channels are activated by PKC [4, 20, 24]. Pretreatment with PKC inhibitors inhibited the late phase of the lactate-induced activation of the H^+ channel, suggesting that PKC might be involved in the activation process. In addition, cell swelling developed slowly in the presence of lower (10–20 mM) concentrations of lactate, which could also contribute to activation of the H^+ channel [22]. As the swelling was not prevented by staurosporine, activation of the H^+ channel might be mediated through different pathways during lactic acidosis.

Patho/physiological implications Tissue disorders are often accompanied by lactic acidosis, cell swelling, depolarization, and fever, all of which activate H^+ channels. Proton channels are rich in the plasma membrane of phagocytes which are involved in the defense mechanism. The activity of NADPH oxidase is pH-dependent and is inhibited by intracellular acidification [31]. Long exposure to lactate depolarized cells to about −10 mV: The H^+ channel would open if pH_i is lower than pH_o by at least ~0.15 U. Additionally, activation of PKC shifts the voltage dependence by about −40 mV [4, 20]. Potentiated H^+ efflux could contribute to a relief of the severe cell acidosis caused by the accumulation of metabolic acid and may hyperpolarize cells. H^+ channels are also essential for charge compensation during the respiratory burst which induces accumulation of intracellular H^+ and depolarization [5, 12, 23]. The activated H^+ channel may serve to maintain phagocytotic action of microglia during long-lasting metabolic acidosis.

Acknowledgements We would like to thank Dr. Charles Edwards for critically reading the manuscript, Y. Moriura and K. Hiraoka for technical assistance, and Y. Yoshioka and M. Okamoto for secretary assistance. This work was supported by a Grant-in-Aid for Scientific Research from The Ministry of Education, Science, and Culture, Japan.

References

1. Byerly L, Meech R, Moody W (1984) Rapidly activating hydrogen ion currents in perfused neurones of the snail, *Lymnaea stagnalis*. J Phyisol 351:199–216
2. Cohen RD, Woods HF (1983) Lactic acidosis revisited. Diabetes 32:181–191
3. DeCoursey TE (2002) Voltage-gated proton channels and other proton transfer pathways. Physiol Rev 83:475–579
4. DeCoursey TE, Chemy VV, Zhou W, Thomas LL (2000) Simultaneous activation of NADPH oxidase-related proton and electron currents in human neutrophils. Proc Natl Acad Sci USA 97:6885–6889
5. Demaurex N, Petheö GL (2005) Electron and proton transport by NADPH oxidases. Philos Trans R Soc B 360:2315–2325
6. Eder C, DeCoursey TE (2001) Voltage-gated proton channels in microglia. Prog Neurobiol 64:277–305
7. Eder C, Fischer HG, Hadding U, Heinemann U (1995) Properties of voltage-gated currents of microglia developed using macrophage colony-stimulating factor. Pflügers Arch 430:526–533
8. Faff L, Nolte C (2000) Extracellular acidification decreases the basal motility of cultured mouse microglia via the rearrangement of the actin cytoskeleton. Brain Res 853:22–31
9. Grinstein S, Furuya W (1988) Assessment of Na^+–H^+ exchange activity in phagosomal membranes of human neutrophils. Am J Physiol 254:C272–C285
10. Grinstein S, Goetz JD, Furuya W, Rothstein A, Gelfand EW (1984) Amiloride-sensitive Na^+–H^+ exchange in platelets and leukocytes: detection by electronic cell sizing. Am J Physiol 247:C293–C298
11. Gordienko DV, Tare M, Parveen S, Fenech CJ, Robinson C, Bolton TB (1996) Voltage-activated proton current in eosinophils from human blood. J Physiol (Lond) 496:299–316
12. Henderson LM, Chappell JB, Jones OT (1987) The superoxide-generating NADPH oxidase of human neutrophils is electrogenic and associated with an H^+ channel. Biochem J 246:325–329
13. Hoffmann EK, Simonsen LO (1989) Membrane mechanisms in volume and pH regulation. Physiol Rev 69:315–382
14. Immke DC, McCleskey EW (2001) Lactate enhances the acid-sensing Na^+ channel on ischemia-sensing neurons. Nat Neurosci 4:869–870
15. Kaila K, Ransom BR (1988) Concept of pH and its importance in neurobiology. In: Kaila K, Ransom BR (eds) pH and brain function. Wiley-Liss, New York, pp 3–10
16. Katsura K, Kurihara J, Siesjo BK, Wieloch T (1999) Acidosis enhances translocation of protein kinase C but not Ca^{2+}/calmodulin-dependent kinase II to cell membrane during complete cerebral ischemia. Brain Res 849:119–127
17. Kreisberg RA (1984) Pathogenesis and management of lactic acidosis. Annu Rev Med 35:181–193
18. Kuno M, Kawawaki J, Nakamura F (1997) A highly temperature-sensitive proton current in mouse bone marrow-derived mast cells. J Gen Physiol 109:731–740
19. Lubec B, Dell'Anna E, Fang-Kircher S, Marx M, Herrena-Marschitz M, Lubec G (1997) Decrease of brain kinase C, protein kinase A, and cyclin-dependent kinase correlating with pH precedes neuronal death in neonatal asphyxia. J Invest Med 45:274–294
20. Mori H, Sakai H, Morihata H, Kawawaki J, Amano H, Yamano T, Kuno M (2003) Regulatory mechanisms and physiological relevance of a voltage-gated H^+ channel in murine osteoclasts: phorbol myristate acetate induced cell acidosis and the channel activation. J Bone Miner Res 18:2069–2076
21. Morihata H, Kawawaki J, Sakai H, Sawada M, Tsutada T, Kuno M (2000) Temporal fluctuation of voltage-gated proton currents in rat spinal microglia via pH-dependent and -independent mechanisms. Neurosci Res 38:265–271
22. Morihata H, Nakamura F, Tsutada T, Kuno M (2000) Potentiation of a voltage-gated proton current in acidosis-induced swelling of rat microglia. J Neurosci 20:7220–7227
23. Murphy R, DeCoursey TE (2006) Charge compensation during the phagocyte respiratory burst. Biochim Biophys Acta 1757:996–1011
24. Nanda A, Grinstein S (1991) Protein kinase C activates a H^+ (equivalent) conductance in the plasma membrane of human neutrophils. Proc Natl Acad Sci USA 88:10816–10820
25. Rehncrona S (1985) Brain acidosis. Ann Emerg Med 14:770–776
26. Ringel F, Chang RC, Staub F, Baethmann A, Plesnila N (2000) Contribution of anion transporters to the acidosis-induced swelling and intracellular acidification of glial cells. J Neurochem 75:125–132
27. Rohra DK, Yamakuni T, Ito S, Saito S, Ohizumi Y (2004) Evidence for the involvement of protein kinase C in acidic pH-induced contraction in spontaneously hypertensive rat aorta. Pharmacology 71:10–16
28. Salimi K, Moser K, Zassler B, Reindl M, Embacher N, Schermer C, Weis C, Marksteiner J, Sawada M, Humpel C (2002) Glial cell line-derived neurotrophic factor enhances survival of GM-CSF dependent rat GMIR1-microglial cells. Neurosci Res 43:221–229
29. Siesjö BK (1988) Acidosis and ischemic brain damage. Neurochem Pathol 9:31–88
30. Siesjö BK, Bendek G, Koide T, Westerberg E, Wieloch T (1985) Influence of acidosis on lipid peroxidation in brain tissues in vitro. J Cereb Blood Flow Metab 5:253–258
31. Simchowitz L (1985) Intracellular pH modulates the generation of superoxide radicals by human neutrophils. J Clin Invest 76:1079–1089
32. Staub F, Beathmann A, Peters J, Weigt H, Kempski O (1990) Effects of lactoacidosis on glial cell volume and viability. J Cereb Blood Flow Metab 10:866–876
33. Thomas RC, Meech RW (1982) Hydrogen ion currents and intracellular pH in depolarized voltage-clamped snail neurons. Nature 299:826–828

2007

J Neural Transm (2007) [Suppl 72]: 113–120

Printed in Austria

Journal of Neural Transmission

Biochemistry of postmortem brains in Parkinson's disease: historical overview and future prospects

T. Nagatsu[1,2], **M. Sawada**[1]

[1] Department of Brain Life Science, Research Institute of Environmental Medicine, Nagoya University, Nagoya, Aichi, Japan
[2] Department of Pharmacology, School of Medicine, Fujita Health University, Toyoake, Aichi, Japan

Summary Biochemical studies on postmortem brains of patients with Parkinson's disease (PD) have greatly contributed to our understanding of the molecular pathogenesis of this disease. The discovery by 1960 of a dopamine deficiency in the nigro-striatal dopamine region of the PD brain was a landmark in research on PD. At that time we collaborated with Hirotaro Narabayashi and his colleagues in Japan and with Peter Riederer in Germany on the biochemistry of PD by using postmortem brain samples in their brain banks. We found that the activity, mRNA level, and protein content of tyrosine hydroxylase (TH), as well as the levels of the tetrahydrobiopterin (BH4) cofactor of TH and the activity of the BH4-synthesizing enzyme, GTP cyclohydrolase I (GCH1), were markedly decreased in the substantia nigra and striatum in the PD brain. In contrast, the molecular activity (enzyme activity/enzyme protein) of TH was increased, suggesting a compensatory increase in the enzyme activity. The mRNA levels of all four isoforms of human TH (hTH1–hTH4), produced by alternative mRNA splicing, were also markedly decreased. This finding is in contrast to a completely parallel decrease in the activity and protein content of dopamine β-hydroxylase (DBH) without changes in its molecular activity in cerebrospinal fluid (CSF) in PD. We also found that the activities and/or the levels of the mRNA and protein of aromatic L-amino acid decarboxylase (AADC, DOPA decarboxylase), DBH, phenylethanolamine N-methyltransferase (PNMT), which synthesize dopamine, noradrenaline, and adrenaline, respectively, were also decreased in PD brains, indicating that all catecholamine systems were widely impaired in PD brains. Programmed cell death of the nigro-striatal dopamine neurons in PD has been suggested from the following findings on postmortem brains: (1) increased levels of pro-inflammatory cytokines such as TNF-α and IL-6; (2) increased levels of apoptosis-related factors such as TNF-α receptor R1 (p 55), soluble Fas and bcl-2, and increased activities of caspases 1 and 3; and (3) decreased levels of neurotrophins such as brain-derived nerve growth factor (BDNF). Immunohistochemical data and the mRNA levels of the above molecules in PD brains supported these biochemical data. We confirmed by double immunofluorescence staining the production of TNF-α and IL-6 in activated microglia in the putamen of PD patients. Owing to the recent development of highly sensitive and wide-range analytical methods for quantifying mRNAs and proteins, future assays of the levels of various mRNAs and proteins not only in micro-dissected brain tissues containing neurons and glial cells, but also in single cells from frozen brain slices isolated by laser capture micro-dissection, coupled with toluidine blue, Nissl staining or immunohistochemical staining, should further contribute to the elucidation of the molecular pathogenesis of PD and other neurodegenerative or neuropsychiatric diseases.

Keywords: Parkinson's disease, postmortem brain, laser micro-dissection, biochemistry, enzymes, cytokines, neurotrophins

Correspondence: Prof. Dr. Toshiharu Nagatsu, Department of Pharmacology, Fujita Health University, Toyoake, Aichi, Japan
e-mail: tnagatsu@fujita-hu.ac.jp

Introduction

The main symptoms of movement disorder, i.e., akinesia, muscle rigidity, and resting tremor, in Parkinson's disease (PD) are caused by a deficiency in the level of the neurotransmitter dopamine at the nerve terminals in the striatum of the nigro-striatal dopamine neurons as the result of selective neurodegeneration of dopamine neurons in the substantia nigra. Most PD is aging-related and sporadic without any hereditary history. Familial PD (PARK) is estimated to represent only ~5% of PD cases. The presence of intracelluar inclusions called Lewy bodies, which are mainly composed of α-synuclein (*α-synuclein* is the causative gene of PARK1), is another feature of sporadic PD. The molecular mechanism of neural degeneration in sporadic PD is speculated to be multiple (Riederer et al., 2001; Nagatsu and Sawada, 2006), involving environmental and/or endogenous potential neurotoxins, oxidative stress, mitochondrial dysfunction, altered iron homeostasis, immune-mediated mechanisms, and susceptibility genes that might be related to the causative genes in familial PD (Mizuno et al., 2006) such as *α-synuclein* or *parkin*. Noradrenaline deficiency in noradrenaline neurons is also observed in the locus coeruleus. These dopamine and noradrenaline deficiencies in the brain of PD patients were first observed by Ehringer and Hornykiewicz (1960). As Foley et al. (2000)

pointed out, Sano et al. (1960, 2000) also observed greatly reduced dopamine levels in the substantia nigra and striatum in one case of postmortem PD brain. This discovery of a dopamine deficiency in the nigro-striatum was a landmark finding of biochemical studies on PD, and led to the development of L-DOPA therapy to supplement the deficient dopamine. L-DOPA was the first neurotransmitter supplementation therapy, and it is still the gold standard of drug therapy for PD.

Up to 1960, even after development of sensitive spectrofluorometric assays, biochemical studies on such unstable compounds as dopamine and noradrenaline had been thought to be difficult to conduct on human postmortem brains. However, after the successful confirmation of the dopamine deficiency in the nigro-striatal region in postmortem PD brains in 1960, biochemical studies on postmortem brains were expanded from various small molecules such as catecholamine neurotransmitters to mRNAs and proteins of enzymes and cytokines related to PD, Alzheimer's diseases (AD), and other neurodegenerative or neuropsychiatric diseases, and have greatly contributed to elucidation of their molecular pathogenesis. This review focuses on the historical development and future prospects of biochemical studies on postmortem brains from PD patients.

Problems in the biochemistry of postmortem brain samples

Biochemical quantitative analyses of human postmortem brain samples have intricate problems, because there are many uncontrollable factors in such samples. The following considerations are generally required in biochemical studies using postmortem brain tissues. (1) Approval of the local ethics committee is essential. (2) Precise clinical information on the patient is required, as drugs administered to the patient may affect primarily or secondarily the level of the compound to be assayed. Most PD patients are administered L-DOPA or dopamine receptor agonists. (3) The condition before death such as the cause of death and the duration of coma may affect the objective compound. No consuming diseases and a short agony stage are necessary conditions to obtain reliable biochemical data. (4) Postmortem time may affect the results. Such compounds as dopamine or noradrenaline are unstable and easily degraded non-enzymatically or enzymatically by monoamine oxidase (MAO). mRNAs and proteins are also unstable. Therefore, the postmortem delay must be as short as possible (preferably within 12 h). (5) Age and postmortem time of PD patients must be similar to those of the control patients. (6) The brain regions to be dissected and the methods of brain dissection should be the same between PD brains and control ones. Punching-out of the micro brain regions from tissue slices (~1–2 cm) is generally used, and the brain location to be dissected out must be the same in each brain sample. As described below, single cell analysis by laser micro-dissection (Hashida et al., 2002; Kawahara et al., 2003) will be a new and valuable method to further our knowledge of the biochemistry of the postmortem brain. (7) Dissected samples should be frozen immediately on dry ice, completely packed and sealed, and stocked at −80° in a deep freezer. (8) Since large numbers of samples are required for proper statistical analysis, a brain bank should be established.

Figure 1 shows schematically the brain bank system in Germany (Riederer P, personal communication).

Changes in catecholamine neurotransmitters and related enzymes in postmortem PD brains

After the discovery of the dopamine deficiency in the nigro-striatum in PD, various neurotransmitters and their related enzymes were measured in postmortem PD brains by us and by other workers. Nagatsu's group first collaborated with Hirotaro Narabayashi (Juntendo University School of Medicine, Tokyo, Japan), who supplied the brain samples from his own brain bank (established by Hirotaro Narabayashi and Reiji Iizuka), and further collaborated with Peter Riederer who established a brain bank at Würzburg University (Würzburg, Germany; Fig. 1).

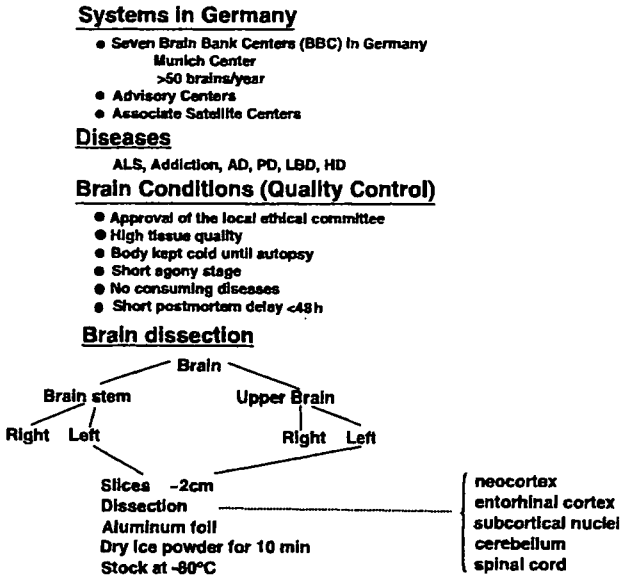

Fig. 1. The brain bank system in Germany (P. Riederer, personal communication)

Table 1. *Changes reported in catecholamine-related enzymes in Parkinson's disease*

Enzymes	Sample source	mRNA	Protein	Activity	Molecular activity (activity/protein)
TH					
Total	striatum		decreased	decreased	increased
Total	SN	decreased	decreased	decreased	increased
hTH1	SN	decreased			
hTH2	SN	decreased			
hTH3	SN	decreased			
hTH4	SN	decreased			
AADC	SN	decreased		decreased	
DBH	CSF		decreased	decreased	normal
	hypothalamus			decreased	
GCH1	striatum			decreased	
PNMT	hypothalamus			decreased	

AADC, aromatic L-amino acid decarboxylase; *CSF*, cerebrospinal fluid; *DBH*, dopamine β-hydroxylase; *GCH1*, GTP cyclohydrolase I; *LC*, locus coeruleus; *PNMT*, phenylethanolamine N-methyltransferase; *SN*, substantia nigra; *TH*, tyrosine hydroxylase.
From Nagatsu et al. (1977, 1981, 1984, 1986), Mogi et al. (1988a, b) and Ichinose et al. (1994).

The results are summarized in Table 1. In our early studies we measured the activities and protein contents of the enzymes related to catecholamine metabolism. We found the presence of phenylethanolamine N-methyltransferase (PNMT) in the control and PD brains, supporting the presence of adrenaline neurons in the human brain (Nagatsu et al., 1977; Trocewicz et al., 1982). We (Nagatsu et al., 1977, 1984) also found a marked decrease (to ~10–20% of controls) in the activity of tyrosine hydroxylase (TH) in the nigro-striatum in PD, in agreement with the results of other workers (Lloyd et al., 1975; McGeer and McGeer, 1976). Riederer et al. (1978) found TH activity to be decreased also in the adrenal medulla in PD, indicating the general impairment of the catecholamine system. DOPA decarboxylase (aromatic L-amino acid decarboxylase, AADC) activity was found to be decreased in the nigro-striatum in PD (Lloyd and Hornykiewicz, 1970). We also found decreased activities in dopamine β-hydroxylase (DBH) for noradrenaline synthesis and PNMT for adrenaline synthesis in PD brains (Nagatsu et al., 1977, 1984). Furthermore, the level of the tetrahydrobiopterin (BH4) cofactor of TH and the activity of the BH4-synthesizing enzyme GTP cyclohydrolase I (GCH1) were found to be decreased in PD brains (Nagatsu et al., 1981, 1986). These results indicate that not only the nigro-striatal dopamine neurons but also all catecholamine neurons are generally affected in PD. Braak et al. (2006) recently proposed, based on the pathology of Lewy bodies, that PD may start in the pre-symptomatic phase from the medulla oblongata where noradrenaline and adrenaline neurons are localized.

The activity of the serotonin-synthesizing enzyme tryptophan hydroxylase (TPH2) was also moderately decreased in the substantia nigra in PD (Sawada et al., 1985). In contrast to PD, in Alzheimer's disease (AD) the activities of TPH2 and TH, and the contents of the biopterin cofactor in the AD brain were found to be moderately decreased in various brain regions, indicating a reduction in the numbers of both serotonin and catecholamine neurons in wide monoamine regions in AD (Sawada et al., 1987).

We examined not only the enzyme activity, but also the protein content measured by enzyme immunoassay, of TH in PD brains. Although both TH protein and TH activity in the nigro-striatum were markedly decreased in parallel in PD brains as compared with those of the control brains, the molecular activity (activity per enzyme protein, also called homo-specific activity) was significantly increased in PD brains. The increase in the molecular activity of residual TH in PD brains suggests that such molecular changes in TH molecules represent a compensatory increase in TH activity (Mogi et al., 1988a). We also measured in cerebrospinal fluid (CSF) of control and PD patients the protein contents and activities of DBH, which synthesizes noradrenaline and adrenaline and is secreted from noradrenaline and adrenaline neurons in the brain into the CSF. In contrast to TH, both DBH activity and protein content in the CSF of PD patients were reduced in parallel ($r = 0.79$) to ~20% of control values without changes in the molecular activity, suggesting only a decreased content in DBH without molecular changes in DBH protein in the noradrenaline and adrenaline neurons in PD (Mogi et al., 1988b). Human TH is markedly activated by the cofactor Fe^{2+}. There are no significant changes in the stimulation of TH activity in the human caudate nucleus by Fe^{2+} in PD, whereas such differences are noted between PD and control brains when exogenous protein kinase is used as a stimulant (Rausch et al., 1988).

Four isoform proteins of human TH (hTH1–hTH4) are expressed by alternative mRNA splicing from a single gene in the brain (Haycock, 2002; Grima et al., 1987; Kaneda et al., 1987; Kobayashi et al., 1988). In human AADC, a single protein is produced by a tissue-specific alternative promoter from neuronal and non-neuronal mRNAs encoded by a single gene (Ichinose et al., 1992). We quantified all four types of human TH mRNAs and AADC mRNA in human brains (substantia nigra) from control, PD, and schizophrenia patients by using the quantitative reverse transcription-polymerase chain reaction (RT-PCR;

Ichinose et al., 1994). All four types of TH mRNAs were detected in the substantia nigra in the control brains examined; and the ratio of hTH1, hTH2, hTH3, and hTH4 mRNAs to the total amount of TH mRNAs was 45, 52, 1.4, and 2.1%, respectively, in the substantia nigra. The levels of TH and AADC mRNAs were highly correlated in the control cases. We found that PD brains had very low levels of all four TH isoform mRNAs and AADC mRNA in the substantia nigra compared with control brains, whereas no significant differences were found between schizophrenic brains and normal ones. We found that monkeys [Japanese monkeys (*Macaca irus* and *Macaca fuscata*), gibbon, orangutan, gorilla, and chimpanzee] have two TH isoforms corresponding to hTH1 and hTH2 (Ichikawa et al., 1990; Ichinose et al., 1993). Monkeys, like humans, are highly susceptible to 1-methyl-4-phenyl-1, 2, 3, 6-tetrahydropyridine (MPTP), a chemical that produces PD in humans (Langston et al., 1983). Thus, we also measured the levels of the two types of TH mRNAs in PD monkeys produced by use of MPTP and compared these levels with those for normal monkeys (Ohye et al., 1995). The levels of both monkey TH mRNAs were significantly decreased specifically in the substantia nigra, which results are similar to those in human PD. All these results indicate that catacholamine-synthesizing enzyme systems are generally decreased in all catecholamine neurons especially in the nigro-striatal dopamine neurons. These decreases may be caused by neuronal degeneration. However, it is not still clear yet when such changes in catecholamine-synthesizing enzymes start in catecholamine neurons in relation to neurodegeneration in sporadic PD. We found that in MPTP-produced animal PD models the changes in the TH system occur soon after MPTP treatment, as evidenced first by a decrease in TH activity, then inactivation followed by a decrease in the protein levels (Nagatsu, 1990).

Presence of MPTP-like neurotoxins in postmortem brains in PD

MPTP inhibits complex I in mitochondria, produces reactive oxygen species, and causes apoptotic cell death in MPTP-induced PD in animals. Dopamine cell death in sporadic PD is also thought to be caused by apoptosis (Hirsch et al., 1999). Since MPTP is a chemically synthesized PD-producing neurotoxin in humans, efforts have been made to find MPTP-like neurotoxins in postmortem PD brains by us and by other workers (Nagatsu et al., 1997, 2002a). Two groups of MPTP-like compounds, isoquinolines (IQs) and β-carbolines, were identified in postmortem human PD brain and in CSF by gas chromatography-mass spectrometry. Similar to MPTP, these IQs and β-carbolines generally inhibit mitochondrial complex I, and cause apoptotic death of catecholamine-producing cells in cultures. Like MPTP, which is converted to toxic 1-methyl-4-phenyl-pyridinium (MPP+) by MAO B, IQs and β-carbolines are also generally N-methylated by N-methyltransferase and then oxidized by MAO B to isoquinolinium ions or carbolinium ions to produce neurotoxicity in animals *in vivo*. Some probable neurotoxins such as (R)-N-Me-salsolinol are assumed to be endogenously synthesized from dopamine in the brain. When (R)-N-Me-salsolinol is administered directly into the striatum in rats, it produces Parkinson-like movement disorders (Naoi et al., 1996). These properties are similar to those of MPP+. The following IQs have been identified in the brain of patients with PD and also of control patients (Nagatsu, 1997; 2002a): tetrahydroisoquinoline (TIQ), 1-Me-TIQ, N-Me-TIQ, N-Me-6,7-(OH)2-TIQ (N-Me-norsalsolinol), 1, N-(Me)2-6,7-(OH)2-TIQ (N-Me-salsolinol), 1-phenyl-TIQ, N-Me-1-phenyl-TIQ, and 1-benzyl-TIQ (1-Bn-TIQ). Among these IQ compounds, 1-Bn-TIQ (Kotake et al., 1995) and (R)-N-methyl-salsolinol (Naoi et al., 1996) are the most potent in producing PD in animals. Among β-carbolines, norharman, harman, 2-Me-norharmanium, and 2,9- (Me)2-norharmanium have been identified in the brain and CSF in normal controls and PD (Collins and Neafsey, 2000; Matsubara, 2000). 1-Trichloromethyl-1,2,3,4-tetrahydro-β-carboline (TaClo) is another neurotoxic β-carboline (Bringmann et al., 2000). Some of these neurotoxins are increased in the brain and/or CSF in PD. However, their distributions in the brain are not specific to the nigrostriatal pathway, and none of them, except MPTP, have been proved to produce PD in humans. Therefore, the significance of these neurotoxins with respect to PD remains unknown.

Changes in cytokines and neurotrophins in postmortem brains in PD

The brain is generally considered to be a "privileged" site, i.e., one free from immune reactions, since it is protected by being behind the blood-brain barrier. However, recent findings revealed that immune responses do, in fact, occur in the brain in PD or in other neurodegenerative diseases, probably by microglia activation that produces pro-inflammatory cytokines (Hayley and Anisman, 2005; Hirsch et al., 2003; McGeer and McGeer, 1995; McGeer et al., 1988; Nagatsu and Sawada, 2005; Nagatsu et al., 1999; Sawada et al., 2006). As described below, PD animals produced by

Table 2. *Changes reported in various cytokines, growth factors, and apoptosis-related factors in Parkinson's disease*

Cytokines, growth factors, or apoptosis-related factors	Tissue studied			
	Substantia nigra	Striatum	Ventricular CSF	Lumbar CSF
TNF-α		increased		increased
IL-1β		increased	increased	increased
IL-2		increased	increased	
IL-4			increased	
IL-6		increased	increased	increased
EGF		increased		
TGF-α		increased	increased	
TGF-β1		increased	increased	
TGF-β2			increased	
NGF	decreased			
BDNF	decreased			
GDNF	no change			
bFGF		no change		
TNF R1 (p55)	increased			
caspase 1 (activity)	increased			
caspase 3 (activity)	increased			
β2-microglobulin		increased		
bcl-2		increased		
solubles Fas		increased		

From Nagatsu et al. (1999) and Nagatsu (2002).

MPTP or 6-hydroxydopamine showed apoptotic death of the nigro-striatal dopamine neurons with increased levels of pro-inflammatory cytokines and decreased levels of neurotrophins. Therefore, we examined changes in the levels of pro-apoptotic cytokines, neurotrophins, and other apoptosis-related factors in the nigrostriatal pathway in postmortem PD brains initially by using the enzyme-linked immunosorbent assay (ELISA; Mogi and Nagatsu, 1999; Mogi et al., 2000; Nagatsu, 2002b; Nagatsu et al., 1999, 2000a, b). Our results are shown in Table 2. We further measured mRNA levels by RT-PCR, and also identified cytokine production by immunohistochemistry at the cellular level (Imamura et al., 2003, 2005; Sawada et al., 2006). We obtained the first ELISA evidence for a marked increase in the level of TNF-α in the brain (striatum) and lumbar CSF (Mogi et al., 1994). This finding was supported by the result of an immunohistochemical study by Boka et al. (1994).

We found that the levels of the following cytokines and apoptosis-related factors in the nigrostriatal pathway, and/or in ventricular and lumbar CSF were elevated: TNF-α, IL-1β, IL-2, IL-4, IL-6, EGF, TGF-α, bFGF, TGF-β1, TNF-β2, Bcl-2, soluble FAS, TNF-α receptor R1 (p55), caspases 1, and 3. We also found decreased levels of neuroprotective neurotrophins, BDNF and NGF, in the substantia nigra. These data on changes in the levels of cytokines in human PD brains were also supported by the results obtained from animal models of PD such as MPTP-treated mice (Mogi et al., 1998) and PD rats produced by injecting 6-hydoxydopamine (Mogi et al., 1999).

Studies on cytokines at the cellular level in the postmortem PD brain: immunohistochemistry and mRNA levels measured by RT-PCR

Inflammatory changes called neuroinflammation, most probably induced by activated microglia, in PD brains have been reported by us and other workers (Angrade et al., 1997; Hirsch et al., 1999, 2003; Jellinger, 2000; McGeer et al., 1988; McGeer and McGeer, 1995; Mogi and Nagatsu, 1999; Nagatsu et al., 1999; Nagatsu and Sawada, 2005; Rogers and Kovelowski, 2003; Sawada et al., 2006). We assume that activated microglia are present in the PD brain to produce pro-inflammatory cytokines and neuroinflammation, ultimately promoting death of dopamine neurons in the substantia nigra. Imamura et al. (2003) of our group identified by Western blot analysis TNF-α and IL-6 proteins in the PD brain. By double immunofluorescence staining, they also proved that ICAM-I- and LFA-1-positive MHC class II-bearing activated microglia in the putamen from sporadic PD patients had produced TNF-α and IL-6 proteins.

Activated microglia and neuro-infammation are observed not only in postmortem brains of patients with sporadic PD, but also in brains of patients with PD caused by MPTP (Langston, 1999) and in MPTP-PD monkeys years after MPTP exposure (McGeer et al., 2003). The question is whether these activated microglia are neuroprotective or neurotoxic toward the nigro-striatal dopamine neurons. Based on the *in vitro* finding of a toxic change from a neuroprotective microglial clone to a toxic one by transduction with HIV-1 Nef protein, resulting in increased NADPH oxidase activity (Vilhardt et al., 2002) and on neuropathological findings of the presence of neurotoxic and neuroprotective subsets of activated microglia in the brains of PD and Lewy body disease (LBD) patients by Imamura et al. (2003, 2005), Sawada has hypothesized that activated microglia may be neuroprotective at least in the initial early stage and may later become neurotoxic by a toxic change during the progression of PD, AD, or other neurorodegenerative diseases (Sawada et al., 2006). This microglia-toxic change hypothesis, if correct, would be expected to be useful for developing drugs against PD. Anti-inflammatory drugs, which are speculated to be useful for the treatment of PD, may inhibit